การเปลี่ยนกลูโคสเป็นกรดลีวูลินิกด้วยตัวเร่งปฏิกิริยาอนุภาคนาโนของคาร์บอนและเหล็กที่ถูกสังเคราะห์จากน้ำมันหล่อลื่นและเฟอร์โรซีน

นางสาวจิรรัตน์ แก้วงาม

วิทยานิพนธ์นี้เป็นส่วนหนึ่งของการศึกษาตามหลักสูตรปริญญาวิศวกรรมศาสตรมหาบัณฑิต
สาขาวิชาวิศวกรรมเคมี ภาควิชาวิศวกรรมเคมี
คณะวิศวกรรมศาสตร์ จุฬาลงกรณ์มหาวิทยาลัย
ปีการศึกษา 2560

CONVERSION OF GLUCOSE TO LEVULINIC ACID BY Fe/CARBON NANOPARTICLE CATALYST SYNTHESIZED FROM LUBRICANT OIL AND FERROCENE

Miss Jirarat Kaewngam

A Thesis Submitted in Partial Fulfillment of the Requirements
for the Degree of Master of Engineering Program in Chemical Engineering
Department of Chemical Engineering
Faculty of Engineering
Chulalongkorn University
Academic Year 2017

Thesis Title	CONVERSION OF GLUCOSE TO LEVULINIC ACID BY Fe/CARBON NANOPARTICLE CATALYST SYNTHESIZED FROM LUBRICANT OIL AND FERROCENE
By	Miss Jirarat Kaewngam
Field of Study	Chemical Engineering
Thesis Advisor	Associate Professor Tawatchai Charinpanitkul, D.Eng.
Thesis Co-Advisor	Sanchai Kuboon, Ph.D.

Accepted by the Faculty of Engineering, Chulalongkorn University in Partial Fulfillment of the Requirements for the Master's Degree

.....Dean of the Faculty of Engineering
(Associate Professor Supot Teachavorasinskun, Ph.D.)

THESIS COMMITTEE

.....Chairman
(Associate Professor Kasidit Nootong, Ph.D.)

.....Thesis Advisor
(Associate Professor Tawatchai Charinpanitkul, D.Eng.)

.....Thesis Co-Advisor
(Sanchai Kuboon, Ph.D.)

.....Examiner
(Associate Professor Varong Pavarajarn, Ph.D.)

.....External Examiner
(Assistant Professor Weerawut Chaiwat, Ph.D.)

จิรรัตน์ แก้วงาม : การเปลี่ยนกลูโคสเป็นกรดลีวูลินิกด้วยตัวเร่งปฏิกิริยาอนุภาคนาโนของคาร์บอนและเหล็กที่ถูกสังเคราะห์จากน้ำมันหล่อลื่นและเฟอร์โรซีน (CONVERSION OF GLUCOSE TO LEVULINIC ACID BY Fe/CARBON NANOPARTICLE CATALYST SYNTHESIZED FROM LUBRICANT OIL AND FERROCENE) อ.ที่ปรึกษาวิทยานิพนธ์หลัก: รศ. ดร.ธวัชชัย ชรินพาณิชกุล, อ.ที่ปรึกษาวิทยานิพนธ์ร่วม: ดร.สัญชัย คูบูรณ์, 81 หน้า.

ในปัจจุบันกระบวนการผลิตกรดลีวูลินิกซึ่งเป็นหนึ่งในสารเคมีที่มีความโดดเด่นเป็นอนุพันธ์ของชีวมวลได้รับศึกษาอย่างมาก ซึ่งชนิดของตัวเร่งปฏิกิริยาที่ถูกนำมาใช้ในการผลิตกรดลีวูลินิกจะอยู่ในกลุ่มจำพวก ซีโอไลท์ โลหะฟอสเฟต และอะลูมินา แต่อย่างไรก็ตามตัวเร่งปฏิกิริยาที่เป็นคาร์บอนที่มีเสถียรภาพต่อความร้อนสูง สามารถปรับปรุงพื้นที่ผิวได้ง่าย มีความทนทานต่อสภาวะที่เป็นกรดและเบส ยังไม่ได้รับการศึกษาอย่างแพร่หลาย ในงานวิจัยนี้จึงได้นำคาร์บอนนาโนพาทิเคิลที่ถูกสังเคราะห์มาจากกระบวนการโคไพโรไลซิสที่มีน้ำมันหล่อลื่นและเฟอร์โรซีนเป็นสารตั้งต้น โดยผลจากการปรับปรุงพื้นที่ผิวด้วยกรดจะศึกษาจากการเกิดคอนเวอร์ชันของกลูโคสและร้อยละผลได้ของกรดลีวูลินิก พบว่าเมื่อใช้ตัวเร่งปฏิกิริยาที่เป็นอนุภาคแมกเนติกนาโนคาร์บอนจะได้ค่าคอนเวอร์ชันของกลูโคสสูงสุดอยู่ที่ 97.58% โดยโมล และได้ร้อยละผลได้ของฟรักโตสอยู่ที่ 26.98% โดยโมล อย่างไรก็ตามในสภาวะนี้จะไม่พบร้อยละผลได้ของกรดลีวูลินิก ในทางกลับกันหากใช้ตัวเร่งปฏิกิริยาที่เป็นอนุภาคแมกเนติกนาโนคาร์บอนที่ผ่านการปรับปรุงพื้นที่ผิวด้วยกรดแล้ว ถึงแม้ว่าจะได้ค่าคอนเวอร์ชันของกลูโคสอยู่ที่ 66.29% โดยโมล แต่จะพบร้อยละผลได้ของกรดลีวูลินิกเท่ากับ 19.52% โดยโมล และไม่พบร้อยละผลได้ของฟรักโตส นอกจากนี้ยังพบว่าเมื่อเพิ่มอุณหภูมิจาก 140ºC ไปจนถึง 220ºC ร้อยละผลได้ของกรดลีวูลินิกจะลดลงเนื่องมาจากปฏิกิริยาข้างเคียงอื่นๆ และพบว่าที่ความเข้มข้นของสารละลายกลูโคส 0.900 กรัม (0.2 M) ปริมาณของตัวเร่งปฏิกิริยาเท่ากับ 0.024 กรัม ที่อุณหภูมิ 180 องศาเซลเซียสและความดัน 21 บรรยากาศ เป็นระยะเวลา 4 ชั่วโมง เป็นเงื่อนไขที่ดีที่สุดที่เหมาะสมสำหรับการทำงานของตัวเร่งปฏิกิริยาอนุภาคแมกเนติกนาโนคาร์บอนที่ผ่านการปรับปรุงพื้นที่ผิวด้วยกรดนี้

ภาควิชา	วิศวกรรมเคมี	ลายมือชื่อนิสิต .....
สาขาวิชา	วิศวกรรมเคมี	ลายมือชื่อ อ.ที่ปรึกษาหลัก .....
ปีการศึกษา	2560	ลายมือชื่อ อ.ที่ปรึกษาร่วม .....

5770382221 : MAJOR CHEMICAL ENGINEERING
KEYWORDS: CARBON NANOPARTICLES, FE/CARBON NANOPARTICLE CATALYST / LEVULINIC ACID PRODUCTION

JIRARAT KAEWNGAM: CONVERSION OF GLUCOSE TO LEVULINIC ACID BY Fe/CARBON NANOPARTICLE CATALYST SYNTHESIZED FROM LUBRICANT OIL AND FERROCENE. ADVISOR: ASSOC. PROF. TAWATCHAI CHARINPANITKUL, D.Eng., CO-ADVISOR: SANCHAI KUBOON, Ph.D., 81 pp.

Currently, production of levulinic acid which is one of promising chemical substances derived from biomass has been intensively investigated. Different catalyst types have been employed to produce levulinic acid from glucose including zeolite, metal phosphate and alumina. However, carbon based catalysts with high thermal stability, ease of surface functionalization and acid-base resistance were not widely studied. In this thesis, carbon nanoparticles synthesized from lubricant oil and ferrocene via co-pyrolysis was fully studied for glucose conversion to levulinic acid. The effect of carbon nanoparticles acid treatment was mainly investigated in terms of glucose conversion and levulinic acid yield. Pristine magnetic carbon nanoparticles (M-CNPs) achieved high glucose conversion of 97.58% (by mole) and fructose yield of 26.98% (by mole). However, none of levulinic acid product could be observed after reaction. On the other hand, the acid treated M-CNPs showed 66.29% (by mole) of glucose conversion and 19.52% (by mole) of levulinic acid yield without detectable fructose product after reaction. The increase of operating temperature from 140^{o}C to 220^{o}C led to the decrease of levulinic acid yield due to the effect of other side reactions. In addition, the optimal condition for levulinic acid production from glucose was obtained at 0.900 g (0.2M) of glucose, 0.024 g of acid-treated M-CNPs, 180 ^{o}C of operating temperature.

Department:	Chemical Engineering	Student's Signature	.....
Field of Study:	Chemical Engineering	Advisor's Signature	.....
Academic Year:	2017	Co-Advisor's Signature	.....

ACKNOWLEDGEMENTS

Firstly, I would like to give my kind gratitude to Assoc. Prof. Tawatchai Charinpanitkul who has advised me and provided my opportunities, including introducing me to National Nanotechnology Center and teaching many lesson in doing my research and living as a successful person. Moreover, I would like to give my thankfulness to my co-advisor, Dr. Sanchai Kuboon, who has taught me many things related to this research, assisted me to use many analytical instruments in NANOTEC, and gave me an opportunity to receive scholarship from TGIST.

Second, I would like to thank Chulalongkorn University. This place has afforded me convenience in doing research and socialization.I kindly thank National Nanotechnology Center (NANOTEC), Thailand Graduate Institute of science and Technology (TGIST) which have provide me a scholar including tuition fee, living stipend, and self-developing expense.

Thirdly, I would like to thanks my family that supported me and stay beside me. They are the inspirers that make me break through the obstacles.

Lastly, I would like to thank my friends. They always listen my problem and be there for me when I need help and pass through the problems with me.

CONTENTS

Page

Chapter 1

1.1 Introduction

Biomass is organic materials that is living or recently living such as agricultural plant and their wastes. Biomass is green feedstock for production of biofuels and chemicals as value-added product and alternative energy. Glucose is the lignocellulosic biomass [1]. It can be converted into the chemical that is the feedstock of the value-added chemicals and materials. Therefore, conversion of glucose is very interesting for improving its worth. At present, production of levulinic acid is one of most interesting chemicals due to many benefits and using in various industrial. Levulinic acid is interested feedstock. There are many researches of levulinic acid production but it is not enough to consume in industrial. Therefore, levulinic acid production was studied continuously. There are 2 main reactions of levulinic acid production. Firstly, homogeneous reaction uses acid liquid catalyst. But this reaction is difficult for separating product from liquid catalyst. Secondly, heterogeneous reaction uses solid catalyst. In this method, products could be separated easily. In addition, kind of catalyst can be modified by many conditions (metal, acid chemicals, solvent, temperature, time, and loading metal)

Levulinic acid is a feedstock for many value-added chemical and material productions. For Biomass program of the USA Department of Energy in 2004 [2], levulinic acid was implied by promising value-added chemical which was desired from biomass. Levulinic acid is chemical intermediate for converting into a large number of chemicals and materials that can be applied by many industries. Therefore, consumption of levulinic acid increased from 450,000 kg per year of consumption in 2000 to 2,600 tons per year in 2013. In the future, consumption of levulinic acid will rose up to 3,800 tons per year in 2020 [2]. For pilot and commercial-scale production of levulinic acid, there are many problems for some process such as the deposition of salt and humins. Thus, acid hydrolysis as

productivity method or cellulosic sugars as substrate was chosen in some process [2]. However, levulinic acid production is not enough for consumption. Therefore, new alternative processes of increasing levulinic acid production are developed.

There are low amount of levulinic acid production. Therefore, new catalyst or new method of synthesizing production were many studied. Heterogeneous catalysis is a very popular technique as industrial process due to many advantages such as easy handing, easy separation and able recycle. Thus, aim of recently studies to find new catalysts that produce levulinic acid.

At present, carbon nanotubes (CNTs) is one of the most popular material because of its special properties [3]. For mechanical properties, It is many-fold stronger than steel, harder than diamond, and higher electrical conductivity than copper. For chemical properties, it can load metal on the surface, modify with oxide group and many functional groups, use in reaction of adsorption and desorption. Resulting, it can be applied to catalyst support, ion adsorbent, electronic conducive paper, fiber, resin, reinforced resin and metal, cell cultivating and drug delivery [4, 5].

Based on literature survey, there is sufficient possibility to employ carbon nanoparticles hybridized with metal component modified by acid treatment for converting glucose to levulinic acid through isomerization, dehydration and rehydration. In order to obtain clear understanding in performance of such hybrized catalysts, there is a need to conduct experimental investigation on conversion of glucose to levulinic acid under controlled conditions. It is recognized that carbon-based materials display good physical and chemical properties. As ideal catalyst supports, multi-walled carbon nanotubes (MWCNTs) were recognized as a good candidate. However, an integration of systematic study in modification of hybridized with iron (Fe) and then application as catalyst for producing levulinic acid from glucose is still unavailable.

In this research, synthesis of CNPs hybridized with Fe and its surface modification via acid treatment were examined. Their catalytically performance testing based on conversion of glucose to levulinic acid was studied. Some new aspects, such as usage of lubricant oil mixed with ferrocene was also examined and discussed in term of CNP production yield. Finally, catalytic activities of CNPs hybridized with Fe for converting glucose to levulinic acid was examined under control conditions. Furthermore, lubricant oil is high consumption and it has extended continuously. 40 million tons per year of lubricant oil consumption around the world was reported by EPA/US. It made about 24 million tons per year of spend lubricant oil. For removed process, regeneration and recycling process are taken to spend lubricant oil. Then, spent lubricant oil is less efficient. It will be taken in energetic assessment or destruction. For this process, there are many problems such as lost energy for thermal combustion and environmental problems. While, co-pyrolysis method is found for removed process for spent lubricant oil. This method is better efficiency to remove spent lubricant oil because main composition of lubricant oil is carbon. Thus, it is used to reactant of co-pyrolysis method. Co-pyrolysis with spent lubricant oil is produced solid, liquid and gas product as fuel and carbonaceous residue. Therefore, carbonaceous residue is interesting because of carbon nanotubes production. Co-pyrolysis method is thermal decomposition method. When heat is taken in co-pyrolysis method, substrate will be destroyed many bonds of substrate leading to produce smaller size of substrate. If it is optimal condition, carbon nanotubes will be produced. Many researchers studied synthesizing condition because of extraordinary properties of carbon nanotubes. Therefore, carbon nanotubes are interesting materials for application.

Co-pyrolysis method is popular for synthesis of carbon nanotubes. It consists of arc-discharge and laser-ablation method. Advantages of co-pyrolysis method are easy handling technique, low cost, enable various substrate (solid, liquid and gas). In addition, carbon nanotubes can growth in various forms and able control with growth parameters. For example, naphthalene was alternative carbon source for synthesis of carbon nanotubes by Charinpanitkul et al., in 2009[6]. For CNTs

precursors, used lubricant oil was collected from industry [7]. Thus, used lubricant oil can be renewable thing that is valued product and value-added waste. Many industries used lubricant oil. Lubricant oil was burnt by combustion for producing thermal energy but it generated environmental pollution. Hence, synthesis of carbon nanoparticles hybridized with Fe nanoparticles via co-pyrolysis would be promising alternatively worth for investigation.

For application of carbon nanotubes, conversion of biomass into biofuel and other chemical feedstocks such as levulinic acid were investigated extensively [1, 7]. Although levulinic acid was produced and developed completely by industrial [8, 9], there were many problems from contamination and by-product. Therefore, levulinic acid production should be investigated continuously for increasing production yield, selectivity and decreasing cost. In this work conversion of glucose to levulinic acid with using carbon nanotubes as catalyst was studied.

Properties of Multi-layer carbon nanoparticles (M-CNPs) hybridized with Fe were characterized by Scanning electron microscope (SEM), Energy dispersive X-ray (EDX), Transmission electron microscope (TEM), Brunauer-Emmet-Teller (BET), Fourier transforms infrared (FT-IR), X-ray diffraction (XRD) and auto titration analyzer. Performance of M-CNPs hybridized with Fe as catalyst was studied by effect of yield and selectivity of levulinic acid production.

1.2 Objective

The objective of this research is to examine conditions for converting glucose to levulinic acid using magnetic carbon nanoparticles hybridized with Fe nanoparticles which were synthesized via co-pyrolysis of lubricant oil and ferrocene for usage as heterogeneous catalyst.

1.3 Scope of research

Scope of this research was designed to cover 3 main parts, which were synthesis of magnetic carbon nanoparticles (M-CNPs) hybridized with Fe nanoparticles via co-pyrolysis, acid treatment and the main part focusing on testing the performance of the synthesized CNPs for converting glucose to levulenic acid. Accordingly, conceptual plan of those parts could be deliberated as follows,

1.3.1 Synthesis of M-CNPs hybridized with Fe nanoperticles via co-pyrolysis of lubricant oil and ferrocene

- Designated condition which based on previous work and literature review were prepared by weight ratio of lubricant oil to ferrocene (2:1), 500^{o}C of decomposition temperature, 900^{o}C of synthesizing temperature, and 30 minutes of residence time with 50 mL/min of carrier gas flow rate.

1.3.2 Acid treatment of M-CNPs hybridized with 8M of nitric acid

Surface of M-CNPs was modified by acid treatment which used nitric acid solution. 0.3 grams of M-CNPs hybridized with Fe was mixed in 70 ml of nitric acid (8 M) and stirred with hot plate for 15 min at 60^{o}C. Preparing mixture was dispersed by ultra-sonication cleaning apparatus for 2 hr. Then, slurry was filtrated by filter membrane and washed by deionized water for remove organic substrates on the surface until neutral pH. After that, this sample was dried in oven at 150^{o}C for 4 hr.

1.3.3 Experimental investigation on performance of the M-CNPs and acid-treated M-CNPs for conversion of glucose to levulinic acid were be conducted.

1.3.3.1 Effect of type of catalyst

Type of catalyst: Commercial CNTs, Fe_3O_4, M-CNPs and Acid-treated M-CNPs

1.3.3.2 Effect of Amount of catalyst

Weight ratio of glucose to a catalyst: 1:1, 3.75:1, 18.75:1, and 37.5:1

1.3.3.3 Effect of reaction Time

Sampling Time: 60, 120, 180, 240 and 300 min

1.3.3.4 Effect of reaction Temperature

Reaction temperature: 140, 160, 180, 200 and 220°C

1.4 Expected benefit

To obtain optimal condition for conversion of glucose to levulinic acid with using magnetic CNPs hybridized with Fe nanoparticles and synthesizing CNPs hybridized with Fe nanoparticles from lubricant oil and ferrocene via co-pyrolysis method.

Chapter 2

Theories and Literature Review

2.1 Levulinic acid

Levulinic acid or 4-oxopentanoic acid is a crystalline compound that is colorless. Properties of levulinic were shown in **Table 2.1**. Levulinic acid is a feedstock of many value-added chemicals because its structure consists of carboxyl group and carbonyl group or ketone group as shown in **Fig. 1**.

Table 2.1 Properties of levulinic acid

Melting point (°C)	33-37
Boiling point (°C)	245-246
Density (g/cm^3)	1.14
pKa @25°C	4.59

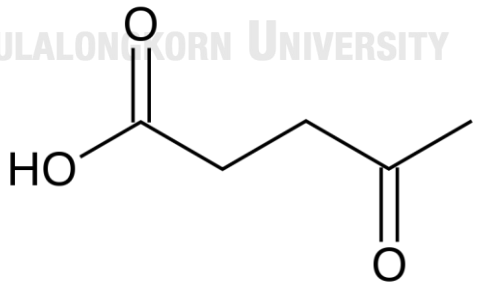

Fig. 2.1 Levulinic acid structure [10].

It can react with other substances to form many chemicals and materials as shown in **Table 2.2**.

Table 2.2 Potential applications of chemicals and productions from levulinic acid

Chemicals	Potentail markets/ application	Chemicals	Potentail markets/ application
Diphenolic acid	Epoxy resins Lubricants Adhesives Paints Polymers	Different esters of LA	Plasticizers Solvents
Succinic acid	Polymers Solvents Pesticides	α-Angelicalactone	Fuel additive Solvents
δ-Aminolevulinic acid	Herbicides Insecticides Cancer treatment	Sodium levulinate	Antifreeze
Methyltetrahydrofuran	Fuel additive Solvents	Calcium levulinate	Antifreeze Pharmaceutical
Ethyl levulinate	Fuel additive Food flavouring	1,4-Butanediol	Polymers Solvents Fine chemicals
γ-Valerolactone (GVL)	Solvents Fuel additives Biofuels Polymers	Valeric (pentanoic) acid	Fuel additive

2.2 Levulinic acid production

Generally, levulinic acid can be produced by derived biomass, such as polymeric carbohydrate (hexose, pentose), alcohol, unsaturated hydrocarbons, 5-methyl furfural, 4-(diphenylmethylsilyl) butyrolactone or nitroethane. Glucose can be isomerized to fructose by Lewis acid sites [11]. Then, dehydrated fructose produce to hydroxymethylfurfural (HMF) with using Brønsted acid catalyst. Rehydrated HMF produce to levulinic acid with using water and Brønsted acid catalyst for opening the ring of HMF at carboxyl group and carbonyl group as shown in **Fig. 2.2**. Thus, Lewis and Brønsted acid sites are impotant in this path way reaction. In addition, Lewis acid sites can decompose glucose to humin but it is not design product [9,14]. This path way is very interesting because fructose can convert to HMF easily.

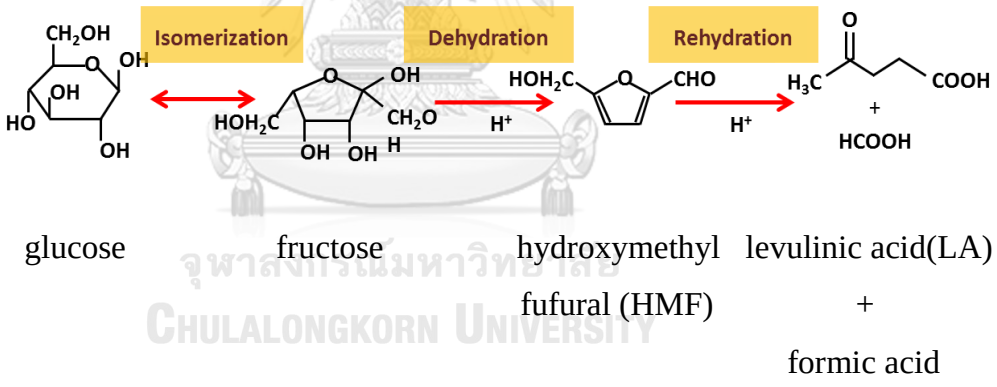

glucose fructose hydroxymethyl fufural (HMF) levulinic acid(LA) + formic acid

Fig. 2.2 Reaction scheme of glucose conversion to levulinic acid [13].

Therefore, properties of catalyst depend on three steps of path way. Firstly, solid catalysts possess Lewis bases because C-O bond of 6-carbon atoms is broken. It became to chain of 6-carbon atoms due to electron from solid catalyst. Secondly, solid catalyst is Brønsted acid catalyst. The chain of 6-carbon atom forms ring of 5-carbon atoms that is fructose and it removes hydroxyl group. Then, hexulofuranose

as intermediate substrate received hydrogen ion from acid catalyst to become HMF. Finally, HMF will be changed to levulinic acid by Brønsted acid catalys.

Levulinic acid production was started from a feedstock and water without catalyst under high temperature and high pressure. Then, dichloromethane (DCM) was added in production process and HCl was replaced DCM which was used to liquid catalyst in levulinic acid production later. Therefore, many inorganics or organic acid compounds can use to liquid catalyst also. HCl and H_2SO_4 are popularly acidic liquid catalyst due to low cost. In addition, Lewis base mixed with acid catalyst and tested to produce levulinic acid. Efficiency of producing levulinic acid is better than only liquid-acid catalyst. After that, condition of acid, neutral and alkaline were studied. Carboxylic acids as reactant under alkaline condition can produce levulinic acid with using liquid acid catalyst. Thus, liquid acid catalyst were popular in that period. In 1956, solid catalyst were used in levulinic acid production process [1]. Solid acid catalysts were studied for levulinic acid production because solid catalyst was easily separated product, function at higher temperature and shortened reaction time and able recycle. Furthermore, solid acid catalyst can modify to improve selectivity. Therefore, solid catalyst is popular for using in industry. However, it stops to find new solid catalyst due to deactivation from a period time and by-product. In addition, modifying catalyst as lanthanide, zirconium and titanium catalysts are toxic and expensive. Recently, $CrCl_3$, $FeCl_3$ and $SnCl_4$ were studied to use for levulinic acid production. Then, an organic-inorganic nanocomposite catalyst was studied in next period.

Many previous reports for levulinic acid production are shown in **Table 2.3**. Levulinic acid production is generated by non-catalyst reaction and liquid catalyst reaction that are called homogeneous reaction and solid catalyst reaction or heterogeneous reaction, respectively.

In 2013, Weingarten gruop studied various ratio of zirconium and tin phosphates. They found 64% of glucose conversion and 22.5% of levulinic acid yield as using molar ratio of phosphorus to zirconium catalyst with 2. Surface area,

total acid site, Brønsted acid sites and ratio of Brønsted to Lewis acid sites were effect of %conversion of glucose and %yield of levulinic acid as shown in **Table 2.4** [12].

Table 2.3 Reaction of conversion of glucose to levulinic acid

Glucose Conc. (wt%)	Solvent	Catalyst	Catalyst Conc.	Temp. (°C)	Reaction/re sident time	Conversion (%)	Yield (%)
30	H_2O	HCl, NaCl	6wt%HCl, 9wt%NaCl	N/A	1,320	N/A	31
2	H_2O	H_2SO_4	1M	140	120	96	38
2	H_2O	H_2SO_4	5wt%	170	120	100	34
30	H_2O	HCl	5wt%	162	60	N/A	24.4
10	H_2O	Zr/P	0.1M	160	180	73	14
1	H_2O	CrCl3+ HY zeolite hybrid	12wt% of substrate	145.2	147	100	47
1	H_2O	CrCl3+ HY zeolite hybrid	1g	160	180	100	62
2	H_2O	$FeCl_3$+ HY zeolite hybrid	1g	180	180	100	62
N/A	H_2O	Zr/P	Solution 70 g	160	180	64	22.5
30	H_2O	GO-SO_3H	0.5 g	200	120	89	78

Table 2.4 Properties of various zirconium and tin phosphates

Cat.	S_{BET} (m^2/g)	Metal(IV) (molar%)	Phosphorus (molar%)	Total $\hat{a}$ sites ($mmol/g$)	Brϕnsted $\hat{a}$ sites ($mmol/g$)	Ratio Brϕnsted to Lewis
ZrP1 P/Zr =1	173	9.45	12.07	1.942	0.240	0.12
ZrP2	276	8.29	16.60	2.146	0.818	0.38
ZrP3	123	8.07	15.95	1.834	0.388	0.21
SnP1	11	9.20	6.64	0.463	0.031	0.07
SnP2	142	11.03	7.20	1.260	0.068	0.05
ZrO_2	143	N/A	N/A	0.905	0.087	0.10

In 2013, Ya'aini et al. studied hybrid catalyst as 1:1, 1:2 and 2:1 weight ratio of $CrCl_3$ to HY zeolite. They found 100% of glucose conversion and 62% of levulinic acid yield as using 1:1 weight ratio of $CrCl_3$ to HY zeolite as hybrid catalyst. Surface area, weak acid and total acid sites for effect of %conversion of glucose and %yield of levulinic acid were shown in **Table 2.5** [13].

In 2015, Ramli et al. studied Fe/HY zeolite catalyst with 5, 10 and 15 weight percent. They found 100% of glucose conversion and 62% of levulnic acid yield as using 10% of Fe/HY zeolite catalyst. Surface area, weak acid and ratio of Brϕnsted to Lewis acid sites for effect of %conversion of glucose and %yield of levuliic acid were shown in **Table 2.6** [10].

According from previous literatures, properties of solid catalyst are significant effect on yield and selectivity of levulinic acid production [13]. Metal-modified CNTs catalysts may point toward high catalytic activity equal the other types of acid catalysts from proper mesopore size that led to higher selectivity to increase levulinic acid yield, higher conversion than the other type of acid catalysts, higher and could be easily separated the reaction products. However, there is one report that is available on carbon nanoparticles catalyzing levulinic production from glucose [9].

Table 2.5 Properties of hybrid $CrCl_3$/HY catalyst

Cat.	S_{BET} (m^2/g)	D_{meso} (nm)	D_{micro} (nm)	HF	Weak $\hat{a}$ (mmol/g)	Moderate $\hat{a}$ (mmol/g)	Total $\hat{a}$ sites ($\mu mol/m^2$)
HY	810	3.90	0.39	0.1522	0.86	0.56	1.75
1:1$CrCl_3$ (w/v%) /HY(g)	393	3.87	0.41	0.1587	0.30	4.86	13.13
1:2$CrCl_3$ (w/v%) /HY(g)	566	3.86	0.40	0.1637	0.40	3.04	9.98
2:1$CrCl_3$ (w/v%) /HY(g)	266	3.87	0.40	0.1568	0.17	2.77	11.05

Table 2.6 Properties of various %Fe in zirconium and tin phosphates:

Cat.	S_{BET} (m_2/g)	D_{meso} (nm)	D_{micro} (nm)	HF	Weak â (mmol/g)	Moderate â (mmol/g)	â sites (μmol/m^2)	Ratio Brønsted to Lewis
HY	829.5	5.86	0.54	0.0716	0.92	0.66	1.91	1.51
5%Fe/HY	598.9	4.33	0.53	0.1371	0.55	2.26	4.69	0.39
10%Fe/HY	549.3	3.77	0.52	0.1532	0.38	2.30	4.88	0.29
15%Fe/HY	522.1	3.62	0.52	0.1626	0.14	1.98	4.06	0.07

2.3 Glucose

Glucose is a monosaccharide that is contained in plant and animal. Glucose consist of six carbon atoms, twelve hydrogen atoms and six oxygen atoms. Its formula is $C_6H_{12}O_6$. It is class of hexose. Glucose can be produced by hydrolysis of carbohydrate. It has been widely used substance for studying lignocellulosic biomass conversion. Conversion of glucose can be occurred by many substances such as 5-hydroxymethyl furfural (5-HMF), levulinic acid and formic acid [16]. Many researches had reported that glucose can be decomposed into fructose to produce 5-HMF, levulinic acid and fructose by homogeneous or heterogeneous reactions.

2.4 Carbon nanotubes (CNTs)

Carbon nanotube (CNT) is a tubular or coaxial cylinder structure that is made of carbon atoms. Diameter of CNTs is nanometer but length of CNTs is micrometers. Covalent sp^2 bonds of CNTs were formed by honeycomb lattice between carbon atoms. CNTs consist of two types that are single-walled carbon nanotube and multi-walled carbon nanotube as shown in **Fig. 2.3**.

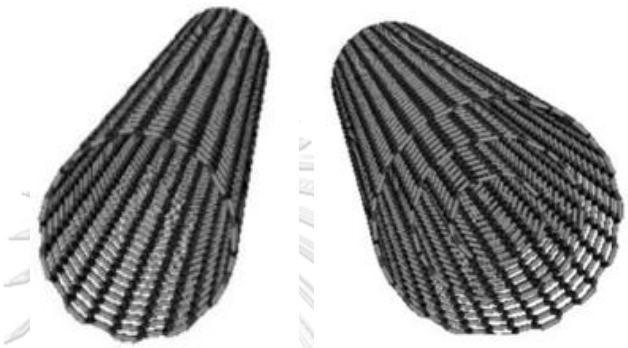

(a) **(b)**

Fig. 2.3 (a) Single-walled carbon nanotube and (b) Multi-walled carbon nanotube [14].

CNTs are recognized a promising material because of extraordinary properties and many potential applications. For mechanical properties, It is many-fold stronger than steel, harder than diamond, and electrical conductivity higher than copper [2]. In 2000, they were found to have a tensile strength of 63 GPa. There are $4x10^9$ A/cm2 electrical current density of CNTs. For chemical properties, it can load metal on the surface, modify with oxide group and many functional groups and react for diffusion, reaction and desorption. As a result, it could be applied in many aspects such as Catalyst support, ion adsorbent, electronic conducive paper, fiber, and resin, reinforced resin and metal, cell cultivating cell and drug delivery system [3, 4].

2.5 Synthesis of carbon nanotubes

CNTs can be synthesized via many methods, such as arc discharge, laser ablation method and chemical vapor deposition (CVD) or co-pyrolysis processes. In arc discharge and laser ablation method, metals or metal salts as the catalysts for synthesis.

Co-pyrolysis is more popular method for synthesis of CNTs because there are many advantages of co-pyrolysis such as simple technique (low temperature, ambient pressure), low cost, various substrates (solid, liquid and gas), easily control growth parameters and various carbon nanotubes form. Therefore, co-pyrolysis is the most popular method of producing CNTs at present. Co-pyrolysis was thermal decomposition of hydrocarbon vapor from reactant which was feed with carrier gas. For liquid hydrocarbon, benzene and alcohol were heated in a flask with inert gas that was purged through reactor. A tubular reactor was heated by tubular furnace that was controlled by temperature controller. When vapor of substrates was feed in reactor, they reacted with metal catalyst to appear self-assembly carbon atoms to form CNTs in reaction zone. Then, products of the CNPs hybridized with Fe were grown on the internal tubular-quartz reactor as shown in **Fig. 2.4**. The product was coated substrates in the hot zone of the reactor to catalyze the growth. Then, the product is collected at room temperature.

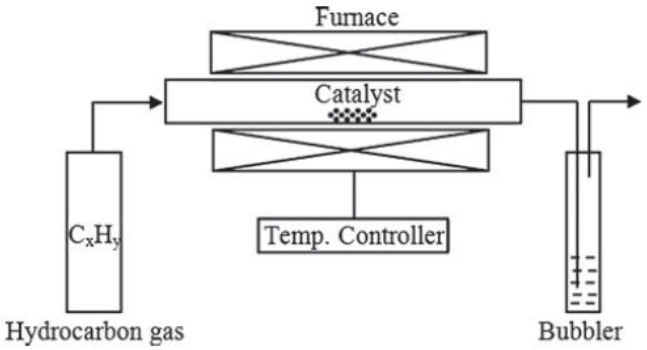

Fig. 2.4 Schematic diagram of CVD setup [14].

For volatile materials such as naphthalene and ferrocene were directly turn from solid to vapor, and perform CVD while passing over the catalyst kept in the high-temperature zone. For CNT growth mechanism has been studied in the past. They found that the reaction conditions are hydrocarbon, catalyst, temperature, pressure, gas-flow rate, deposition time, reactor geometry. They are affected on the CNTs growth. Generally, there are 2 kinds of the growth mechanisms. When hydrocarbon vapor comes in contract with the hot metal nanoparticles, substrate is decomposed into carbon and hydrogen atoms. Then, hydrogen will be decomposed and carbon atoms will be dissolved into the metal. If the catalyst-support interaction is weak. Metal has an acute contact angle with the substrate. Then, metal particle is displaced from the surface hydrocarbon decomposes on the top surface of metal, carbon diffuses down through the metal (concentration gradient exists in the metal allowing carbon diffusion), and CNT precipitates out across the metal bottom, pushing the whole metal particle off the substrate by the carbon tip-growth mechanism. The metal's top is open for fresh hydrocarbon decomposition, then the carbon tubes grow longer and longer away from the support surface. When the metal is fully covered with excess carbon, its catalytic activity ceases and the CNT growth is stopped. If interaction of catalyst-support is strong (metal has an obtuse contact angle with the substrate) as be called base-growth mechanism, initial hydrocarbon decomposition and carbon diffusion take place, but CNT precipitation fails to push the metal particle up. Therefore, the CNT precipitation is compelled to emerge out from the metal's apex. Carbon crystallizes can out as a dome and extends up in the form the graphitic cylinder. Therefore, hydrocarbon deposition is taken place on the lower surface of the metal, and as dissolved carbon diffuses upward. Then, CNT grows up with the catalyst on its base. These growth mechanisms have been further simplified by Moisala et al. as shown as **Fig. 2.5** [15].

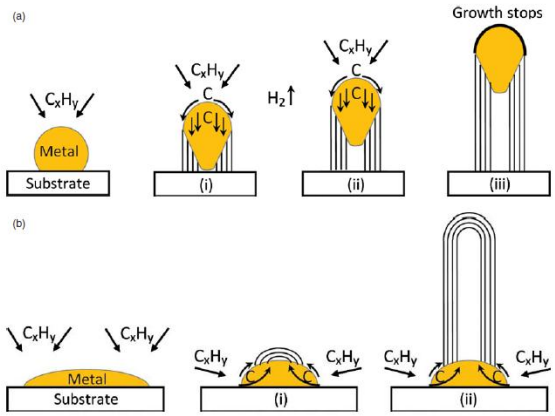

Fig. 2.5 Widely-accepted growth mechanism for CNTs: (a) tip-growth model, (b) base-growth model [14].

2.6 Acid treatment of carbon nanotubes

Acid treatment is the most method for CNTs oxidation. Purity and addition of functional group on surface of carbon nanotubes were improved by using acid treatment. HNO_3, H_2SO_4 and $KMnO_4$ are popular acids for acid treatment. Acids and solid catalyst were mixed and taken high sonication for dispersing nanotubes in acid solution [16]. For acid treatment, the interfacial bonding is promoted because the wet-oxidation is appeared. Hydroxyl, carbonyl and ketone groups (OH, COOH, and C=O) can be introduced on multi-walled carbon nanotubes in liquid-phase of oxidation method. Nitric acid is used to oxidize MWCNTs for 48 hr and Hiura et al. reported that mixture of nitric acid and sulfuric acid were applied with potassium permanganate for more than 5 hr. They can purify and oxidize carbon nanotubes [17]. Single-walled CNTs were treated in hot nitric acid. It can lead elimination of metal impurities and amorphous carbon. This information was found by Hu group and Martinez group in 2003 [17, 18]. Datsyuk group studied chemical oxidation of MWCNTs that treated with acid and base of oxidative treatments on the MWCNTs They were produced by chemical vapor deposition method [19]. After acid treatment, density of carboxyl and hydroxyl group on the MWCNTs increased on surface of MWCNTs.

Chapter 3

Experimental

In this work, experiment consists of three parts. Firstly, M-CNPs hybridized with Fe were synthesized by lubrication oil, ferrocene and acid treatment via co-pyrolysis. Secondly, characterization of hybridized CNPs with Fe was determined by FE-SEM, TEM, BET, FT-IR, TGA, auto titration and AAS. Finally, catalytic performance test of M-CNPs hybridized with Fe for conversion glucose to levulinic acid was analyzed by HPLC to determine glucose conversion and levulinic yield.

3 Experimental works

3.1 Synthesis of M-CNPs hybridized with Fe via co-pyrolysis

3.1.1 Materials

- Commercial Diesel Lube oil from Shell company, Gelix HX5 15W-40
- Ferrocene ($Fe(C_5H_5)_2$) from Sigma-Aldrich, ≥98% of Fe
- Nitrogen gas(N_2) from LINDE, 99.999% of purity
- Commercial CNTs (baytubes C150 P) from Bayer MaterialScience

3.1.2 Procedure

- Ratio of ferrocene and lubricant oil was 1:2 (by weight). They were prepared and mixed by Ferrocene 1 gram and lubricant oil 2 grams. The mixture was taken in boat container which was placed in the tubular quartz reactor at lower temperature zone. Two temperature zones were set by two controllers of two tubular furnaces. First furnace was set temperature at 500°C and the second furnace was set temperature 900°C. Equipment was shown in the **Fig. 3.1**. When the temperature increased to optimize setting condition, the tubular quartz reactor was pushed into the optimize position. Nitrogen gas was flowed 50 ml/min. There is 30 minutes as

the residence time. After the tubular was cooled, the product was collected. Then, it was dried in the oven overnight at 60°C.

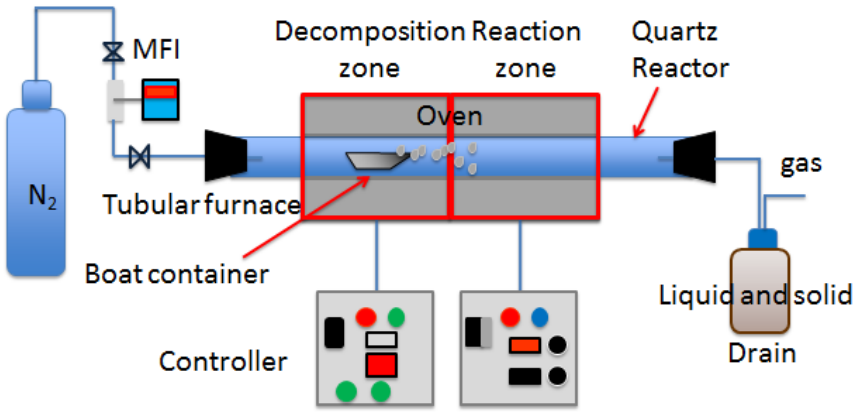

Fig. 3.1 Scheme of reactor for synthesis of Fe-CNTs via chemical vapor deposition method

3.2 Acid treatment of CNPs hybridized with Fe with 8M of nitric acid

3.2.1 Materials

- M-CNPs hybridized with Fe via co-pyrolysis
- Nitric acid (69%w/w, D= 1.51 g/cm^3, M.W.63.01g, UNIVAR)
- Deionized water

3.2.2 Procedure

Surface of M-CNPs were modified the acid treatment by nitric acid solution. The 0.3 g of M-CNPs were mixed in a 70 ml of nitric acid (8 M) by hot plate stirrer for 15 min at 60ºC. They were dispersed by ultrasonic cleaning apparatus for 2 hr. Then, the slurry was filtrated by membrane filter and washed with deionized water to remove organic substrates on the surface until neutral pH of water. After that, sample was dried in oven at 150ºC for 4 hr.

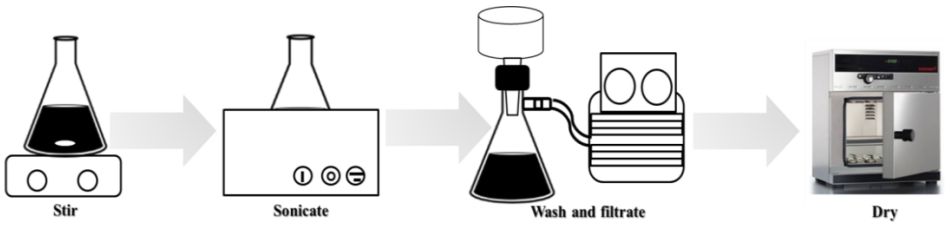

Fig. 3.2 Acid treatment method

- Characterization:

- Field emission scanning electron microscope (FESEM, JEOL JSM-7800F, Japan) as shown in **Fig. 3.3** were employed for analyzing commercial CNTs, synthesized products from zone A, B, C, D and remaining product from synthesis. Various elements of the commercial CNTs and M-CNPs were analyzed by Back-scattered electron detector (BSC/FE-SEM). Different ratio of elements of M-CNPs and acid-treated M-CNPs were analyzed by Energy dispersive X-ray spectroscopy (FE-SEM/EDX).
- Morphology of internal structure of commercial CNTs, M-CNPs and acid-treated M-CNPs were characterized by transmission electron microscope (TEM, JOEL JEM2100) as shown in **Fig. 3.4**. Solid samples were prepared in ethanol for dispersion. Then, substances were floated on surface of solvent. They were kept on plates to analyze.
- Porosity and specific surface area, average pore size distribution and total pore volume of the commercial CNTs, synthesized products from zone A, B, C, D and acid-treated M-CNPs were analyzed by N_2 sorption based on Barrett-Joyner-Halenda (BJH) method, and micro and meso porosity based on Brunauer-Emmet-Teller (BET, Belsorp-Mini, Bel Japan) via t-plot method as shown in **Fig 3.5**. 0.02 grams of samples were pretreated at 120^{o}C for 8 hr before they were analyzed by BET.
- Graphitic and disorder structure of the commercial CNTs, synthesized products from zone B, C, D and acid-treated M-CNPs were analyzed by Raman spectrometer (NT-MDT, Rassia) with an invert confocal microscope

(Olympus IX71, USA) and a cooled CCD detector at 60^{O}C as shown in **Fig 3.6**. Excited wavelength of He-Ne laser was 532 nm as 100X objective lens with laser power. Samples were trapped on glass slides and were taken on stage of microscope for analyzing.

- CHN result of lubricant oil, commercial CNTs and M-CNPs were obtained the carbon, hydrogen and nitrogen percentages by Carbon-hydrogen-nitrogen elemental determinator (The CHN 628 series, from LECO Corp., US) as shown in **Fig. 3.7**. 0.1 gram of samples were wrapped by aluminium foil. Then, they were taken in the auto sampling of the CHN analyzer to combust, detect and analyze.
- Atomic absorption spectroscopy (AAS, Model AA280FS, Varian) was used to analyze amount of iron of commercial CNTs, M-CNPs and acid-treated M-CNPs in mg/L.
- Purity and the compositions in the M-CNPs and acid-treated M-CNPs were analyzed by Thermal gravimetric analysis (TGA, NETZSCH, STA 449 F5 Jupiter) as shown in **Fig. 3.8**.
- Functional group and acid group on the surface of the commercial CNTs, M-CNPs and acid-treated M-CNPs were analyzed by Fourier transforms infrared (FT-IR, Nicolet 6700, Thermo Scientific) **as shown in Fig 3.9** and used spectra with a nominal resolution of 4 cm^{-1} in range of 500-4000 cm^{-1} at room temperature.
- Acidity of acid of the commercial CNTs, M-CNPs and acid-treated were analyzed by Automatic titration (T50, Mettler Toledo) as shown in **Fig 3.10**.

- Equipment for Characterization:

Fig. 3.3 Field emission scanning electron microscope

Fig. 3.4 Transmission electron microscope

Fig. 3.5 Brunauer-Emmet-Teller 32

Fig. 3.6 Raman spectrometer

Fig. 3.7 Carbon-Hydrogen-Nitrogen elemental exterminator

Fig. 3.8 Thermal gravimetric analysis

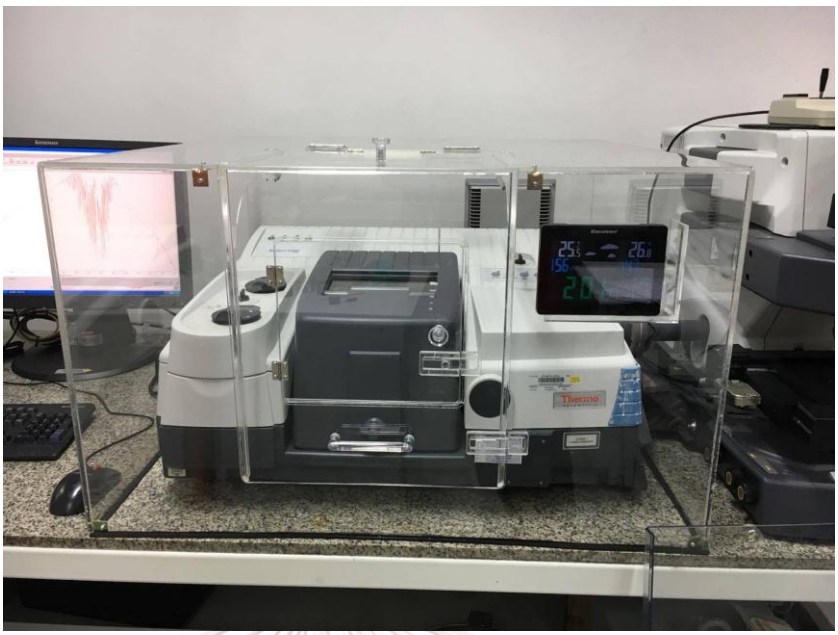

Fig. 3.9 Fourier transforms infrared

Fig. 3.10 Automatic titration

3.3 Performance testing

Performance testing is main part of this work. Effect of temperature, time and amount of catalyst loading will be experimentally examined. In addition, fresh catalyst and spent catalyst were characterized and tested in comparison with other carbonaceous materials, such as commercial CNTs.

3.3.1 Materials

- D(+)-glucose monohydrate (MW.180 g/mol)
- Deionized water
- Commercial CNTs (baytubes C150 P) from Bayer MaterialScience
- CNPs hybridized with Fe via co-pyrolysis
- A Standard analytical grade of hydroxymethylfurfural(HMF)
- A Standard analytical grade of levulinic acid 98%

3.3.2 Procedure

One pot catalytic reaction was carried out by dissolving of glucose in deionized water and it was mixed by catalyst in a closed 130 ml of Autoclave with various conditions as shown in **Table 3.1**. Then, reaction system control desired temperature and time with stirring speed for 300 rpm. All samples are filtered by 0.22 μm of membrane syringe filter. Liquid phase was analyzed by high performance liquid chromatography (HPLC) (Shimadzu UFLC) as shown in **Fig. 3.11**. Column was organic acid Aminex HPX-87H that was 45°C of temperature. Mobile phase was H_2SO_4 (5mM) that was 0.6 mL/min of flow rate. Detector was UV 210 nm and retention time was 80 min. Glucose conversion, product yield and selectivity were calculated by **Eqs. (1)-(3)**;

Glucose conversion (%)

$$= \frac{\text{Initial glucose (mol)-Final glucose (mol)}}{\text{Initial glucose (mol)}} \times 100\% \quad (1)$$

Product yield (%)

$$= \frac{\text{Amount of product (mol)}}{\text{Initial glucose (mol)}} \times 100\% \qquad (2)$$

Selectivity (%)

$$= \frac{\text{Desired product (mol)}}{\text{Undesired product (mol)}} \times 100\% \qquad (3)$$

Fig. 3.11 High performance liquid chromatography

Table 3.1 Effect of catalyst types in each condition

Effect of	Types of catalysts	Amount of catalyst	Reaction Time	Temperature
Types of catalyst	Commercial CNTs Fe_3O_4 M-CNPs Acid-treated M-CNPs	Acid-treated M-CNPs	Acid-treated M-CNPs	Acid-treated M-CNPs
Concentration of glucose	0.48 g (0.1 M) in 50 mL of solution	0.9 g (0.2 M) in 25 mL of solution	0.9 g (0.2 M) in 25 mL of solution	0.9 g (0.2 M) in 25 mL of solution
Reaction Temperature	160°C	160°C	160°C	140, 160, 180, 200 and 220 °C
Pressure gauge	1 atm	21 atm	21 atm	21 atm
Sampling Time	30, 60, 90, 120, 150 and 180 min	120 min	60, 120, 180, 240 and 300 min	240 min
Weight ratio of glucose to catalyst	1	1, 3.75, 18.75, 37.5	37.5	37.5

Chapter 4

Results and discussion

4.1 Synthesis of M-CNPs hybridized with Fe nanoperticles via co-pyrolysis of lubricant oil and ferrocene

Magnetic CNPs hybridized with Fe or M-CNPs could be synthesized from lubrication oil and ferrocene via co-pyrolysis. A quartz tube reactor employed in this work was divided into 4 sections as shown in **Fig. 4.1.** In order to regulate temperature profile, the reactor was heated by a set of 2 electrical furnaces. **Fig.4.2** illustrates a standard temperature profile used in this work.

In zone A, typical product was collected from a location situated in the first furnace with an average temperature of 578°C. The length of zone A is along an axial distance of 0-30 cm. In zone B, the product was collected from the location which was also situated in the first furnace with average temperature of 788°C along an axial distance of 30-45 cm. In zone C, the product was collected from the location situated in the second furnace with average temperature of 906°C. This

zone is along an axial distance of 45-75 cm. In zone D, the product was collected from the location which is also situated in the second furnace with lower average temperature of 768°C and its dimension along an axial distance is 75-120 cm.

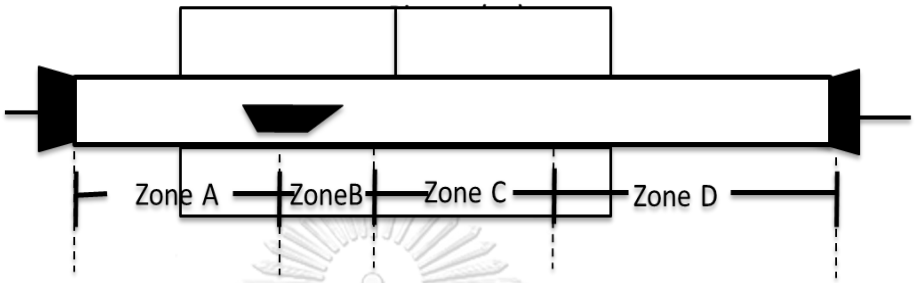

Fig. 4.1 The sections of product collecting in each zone that were referenced with the length of the quartz tube reactor

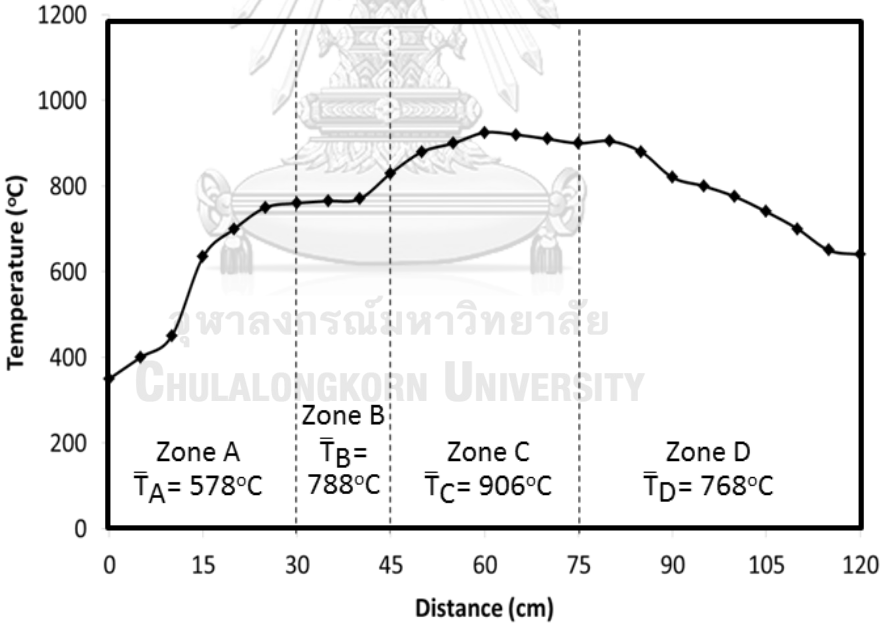

Fig. 4.2 Temperature profile of 2-temmperature-zone co-pyrolysis system for synthesizing M-CNPs on quartz tube reactor.

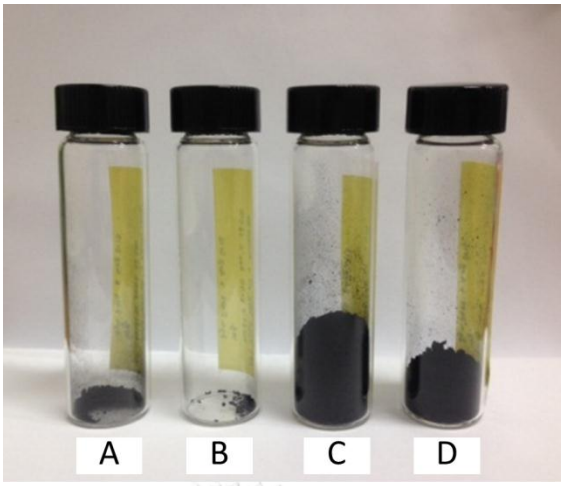

Fig. 4.3 Optical images of collected product in quartz reactor from co-pyrolysis of lubricant oil and ferrocene (A) the product zone A (B) the product zone B, (C) the product zone C and (D) the product zone D

Appearance of typical product collected from each zone was shown in **Fig. 4.3**. The amount of product collected from zone C was the major portion with the highest quantity. As mentioned above, zone C is situated the second furnace with an average temperature of 900ºC. Then highest product portion in this zone was attributed to formation of synthesized CNPs under balancing effect of flow rate of carrier gas and reaction temperature [6]. This carrier gas flow rate was 50 ml/min. It was proper for carrying the amount of reactant into the reaction zone with temperature proper for self-assembly of CNTs.

Field-emission scanning electron microscopy (FE-SEM) was employed to investigate morphology of the commercial CNTs, products collected from each zone of the quartz tube reactor (**Fig. 4.4-4.6**). From **Fig. 4.4 (a) and (b)**, it could be clearly observed that the commercial CNTs exhibited tubular morphology with rather uniform diameter of 10 nm. There were only few residual spherical nanoparticles within the sample of the commercial CNTs.

For product samples collected from zone A, they consisted of irregular tubular particles with nominal diameter of 38-112 nm as shown in **Fig. 4.5 (a1) and (a2)**.

According to **Fig. 4.5 (b1) and (b2)**, some carbon nanotubes mixed with amorphous carbon nanoparticles could be observed in typical samples collected from zone B.

Meanwhile, in zone C carbon nanotubes with nominal diameter of 40-60 nm existed uniformly as shown in **Fig. 4.5 (c1) and (c2)**.

The product samples collected from zone D were shown in **Fig. 4.5 (d1) and (d2)**. A mixture of CNTs and irregular nanoparticles with carbonaceous and metallic content could be observed. It should be noted that in this zone the average temperature was lower due to heat loss.

Based on SEM analyses, products in zone C exhibited more uniform tubular structure when compared to those of zones B and D. These results would be attributed that in a high temperature zone, the self-assembly process to provide CNTs would be dominant [7]. In zone B with a lower temperature, only few CNTs were observed because the self-assembly process would be in premature stage. On the other hand, the convective flow of carrier gas would carried over some CNTs to zone D where only some remaining carbon clusters would undergo the self-assembly process to form only a few CNTs.

Finally, it was considered that product from zone C was the most promising because of the best characteristics of CNTs. In this work, the product collected from zone C is called “magnetic carbon nanoparticles (M-CNPs)”. Based on TEM analysis (available in **Fig. 4.11**), average inner diameter of these M-CNPs was 10-20 nm and average outer diameter was 40-60 nm. Some iron nanoparticles were randomly dispersed in M-CNPs. A trend of average diameter of M-CNPs collected from zone C is in an acceptable agreement with particle size analysis which will be reported discussed later.

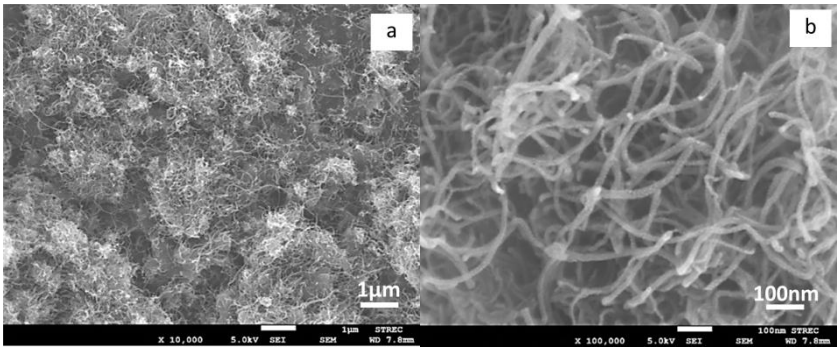

Fig. 4.4 FE-SEM images of commercial CNTs at different magnification (a) 10,000 × (b) 100,000 ×

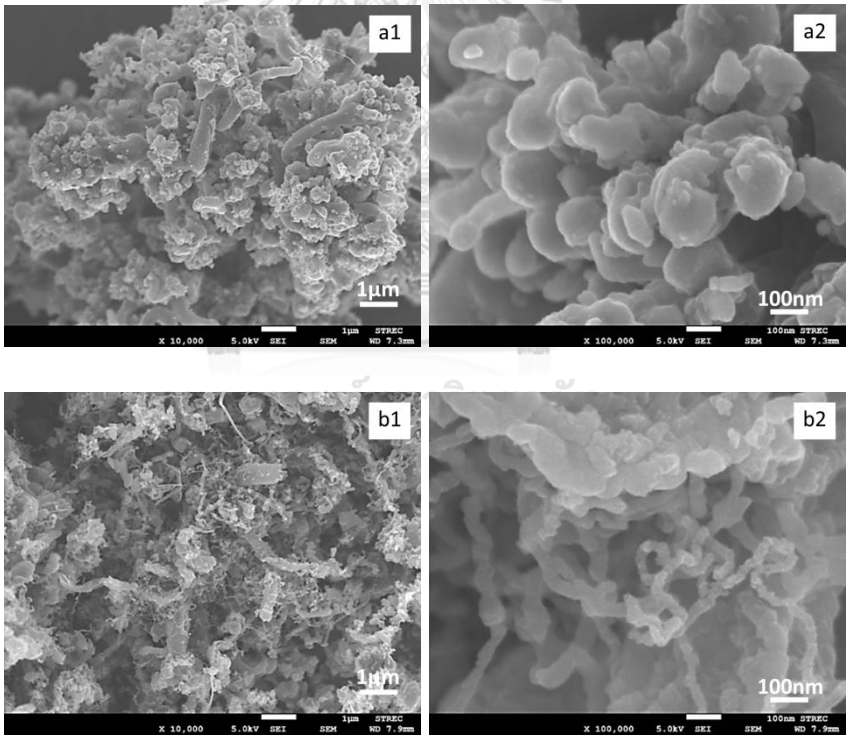

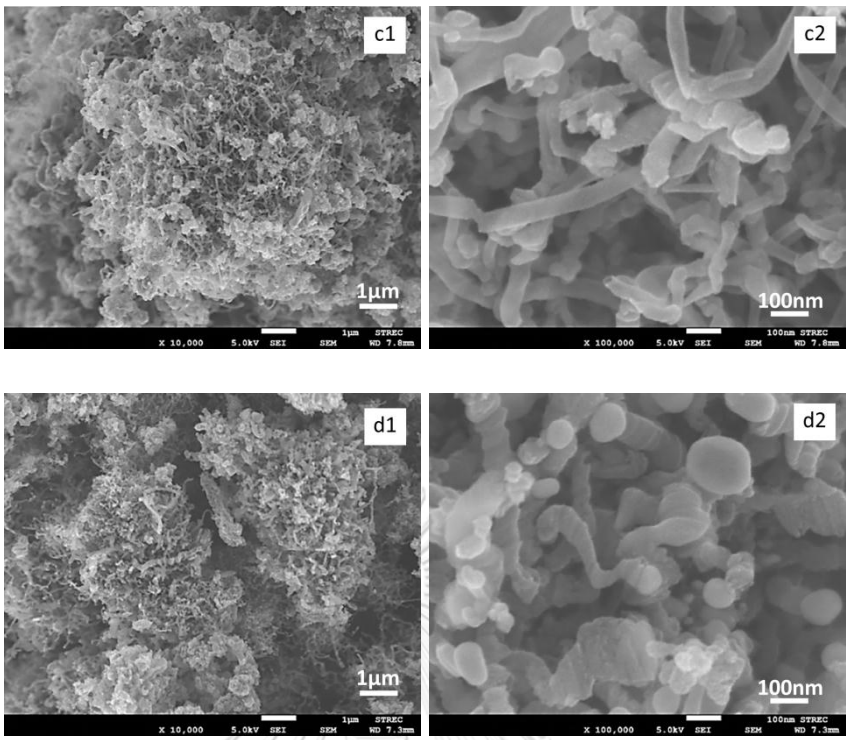

Fig. 4.5 FE-SEM images of collected product in quartz reactor from pyrolysis (a1) the product of zone A magnitude 10,000 × (a2) magnitude 100,000 ×, (b1) the product of zone A magnitude 10,000 × (b2) magnitude 00,000 × and (c1) the product of zone D magnitude 10,000 × (c2) magnitude 100,000 ×

For the **Fig. 4.6 (a)**, it was shown the product out of the quartz reactor. There were the least size of diameter than other zone, but they are mixed with a large of carbonaceous and iron nanoparticles.

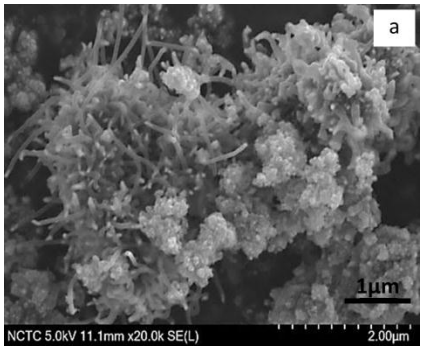

Fig. 4.6 SEM images of collected product from particulate collector.

From the FE-SEM result, the tubular structure was not appeared in the product from zone A and there were a lot of carbonaceous particles than tubular structure in the product out of the quartz tube reactor. After that, the synthesized products were analyzed by nitrogen adsorption isotherms and textural properties of commercial CNTs and the product in each zone as shown in **Table 4.1** for supporting information. Because of the next step for catalytic conversion of glucose, the surface area is the one of important factor in heterogeneous reaction.

Table 4.1 The Brunauer-Emmett-Teller (BET) surface area, total pore volume and average pore diameter of commercial CNTs and the product synthesized at zone A, B, C and D

Samples	a_s,BET ($m^2 \cdot g^{-1}$)	Total pore volume ($cm^3 \cdot g^{-1}$)	Avg. pore diameter (nm)
Commercial CNTs	221±6	0.48±0.15	8.88±2.68
The product from zone A	17±3	0.01±0.01	3.01±1.15
The product from zone B	24±1	0.04±0.02	6.58±2.74
The product from zone C	43±3	0.06±0.01	4.58±0.15
The product from zone D	50±5	0.06±0.002	4.80±0.14

The table was shown that the surface area of the product from each zone was significant decrease when they were compared with the commercial CNTs. In addition, the total pore volume and average pore diameter of the product in each

zone was less than CNTs. For difference in each zone, it found that the surface area, total pore volume and average pore diameter of the product from zone C and D was higher than zone A and B because of the decreasing of CNTs' diameter.

Thus, the product in zone A was cut out of the next analysis because of the morphology from FE-SEM and the information from BET analysis. The product in zone A was not proper for being catalyst in the heterogeneous reaction.

The Raman spectra of commercial CNTs, product of zone B, the product of zone C and the product of zone D were monitored at over 1,000-3,000 cm^{-1} to characteristic of the C-C bond vibration mode of multi-walled CNTs (MWCNTs) as shown in **Fig. 4.7**. The Raman spectra of CNTs was shown a peak at 1,335 cm^{-1} as a D band, and peak at 1,572 cm^{-1} as G band, whereas the peak at 1,340, 1,345 and 1,345 cm^{-1} as a D band, and a peak at 1584, 1,579 and 1,586 cm^{-1} as G band from the spectra of the product zone B, C and D. The G peaks were shown that crystal structure of them. The D peaks were shown that amorphous structure of them. From data, G and D peaks the product of zone C or in the second furnace temperature 900ºC, at 45-75 cm was the same as the commercial CNTs as shown in **Table 4.2**. That was shown that the product in the second furnace temperature 900ºC, at 47-45 cm was more crystalline than from other distances in quartz reactor. Addition, The intensity of spectra at temperature 500ºC is lower than 900ºC because it would be decomposed completely and well-formation at higher temperature than lower temperature. In addition, the image results from FE-SEM from **Fig.4.4** and **Fig.4.5** was supported by the intensity of G and D peaks that the formation of product in zone C was interesting product for application.

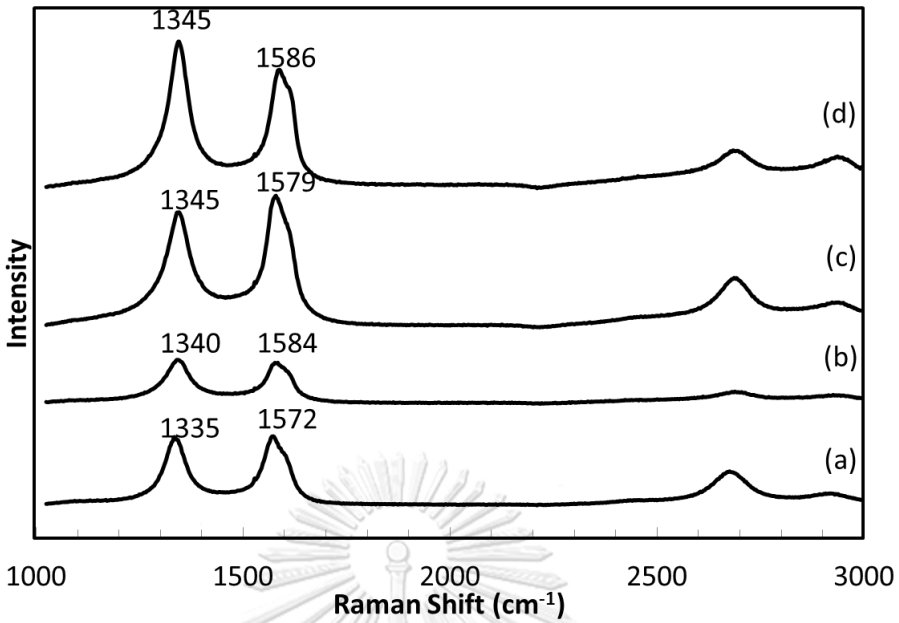

Fig. 4.7 Raman spectrum of (a) commercial CNTs and product synthesized at (b) zone B, (c) zone C and (d) zone D

Table 4.2 The ratio between I_D and I_G of commercial CNTs, and the product form zone B, C and D

Element	I_D/I_G
Commercial CNTs	0.954
CNPs zone B	1.070
CNPs zone C	0.915
CNPs zone D	1.218

From the FE-SEM, BET and Raman analysis, the product from zone C was used to study in the next step. This product was called Magnetic carbon nanoparticles hybridized with Fe (M-CNPs) due to ability to attract by magnet and impurities that were mixed with carbon nanotubes.

The interested product yield after investigation the product in differs interested distances in reactor was listed in **Table 4.3**, it was shown that the interested product yield was about 14.20 – 15.52% $\pm$ 0.61. The remaining percentages were amorphous, many clusters and removal particles in other zones. The standard deviation was confirmed the repeatability for production of M-CNPs.

Table 4.3 Yield of M-CNPs at zone C of reactor

Samples	Batch 1	Batch 2	Batch 3	Batch 4	SD
M-CNPs Weight (g)	0.4688	0.4318	0.4537	0.4354	0.0172
Lubricant oil and Ferrocene Weight (g)	3.0211	3.0418	3.0053	3.0223	0.0150
Yield(%)	15.52	14.20	15.10	14.41	0.61

The CHN result of lubricant oil, commercial CNTs and interested product (M-CNPs) were listed in **Table 4.4**, carbon percent of lubricant oil was 55.45%±3.80 as shown that the compositions of the lubricant oil were carbon and other element. Thus, that was the cause of the low of yield. In addition, the main composition of the M-CNPs was the carbon. It was shown that when lubricant oil was decomposed, the most of carbon particles were formed into M-CNPs.

Table 4.4 The CHN analysis of lubricant oil, commercial CNTs and M-CNPs.

Samples	Nitrogen (%)	Carbon (%)	Hydrogen (%)
Lubricant oil	0.06 ±0.02	55.45 ±3.80	8.81 ±0.4 0
Commercial CNTs	0.07 ±0.08	97.44 ±0.20	0.38 ±0.04
M-CNPs	0.40 ±0.03	76.87 ±6.00	0.61 ±0.07

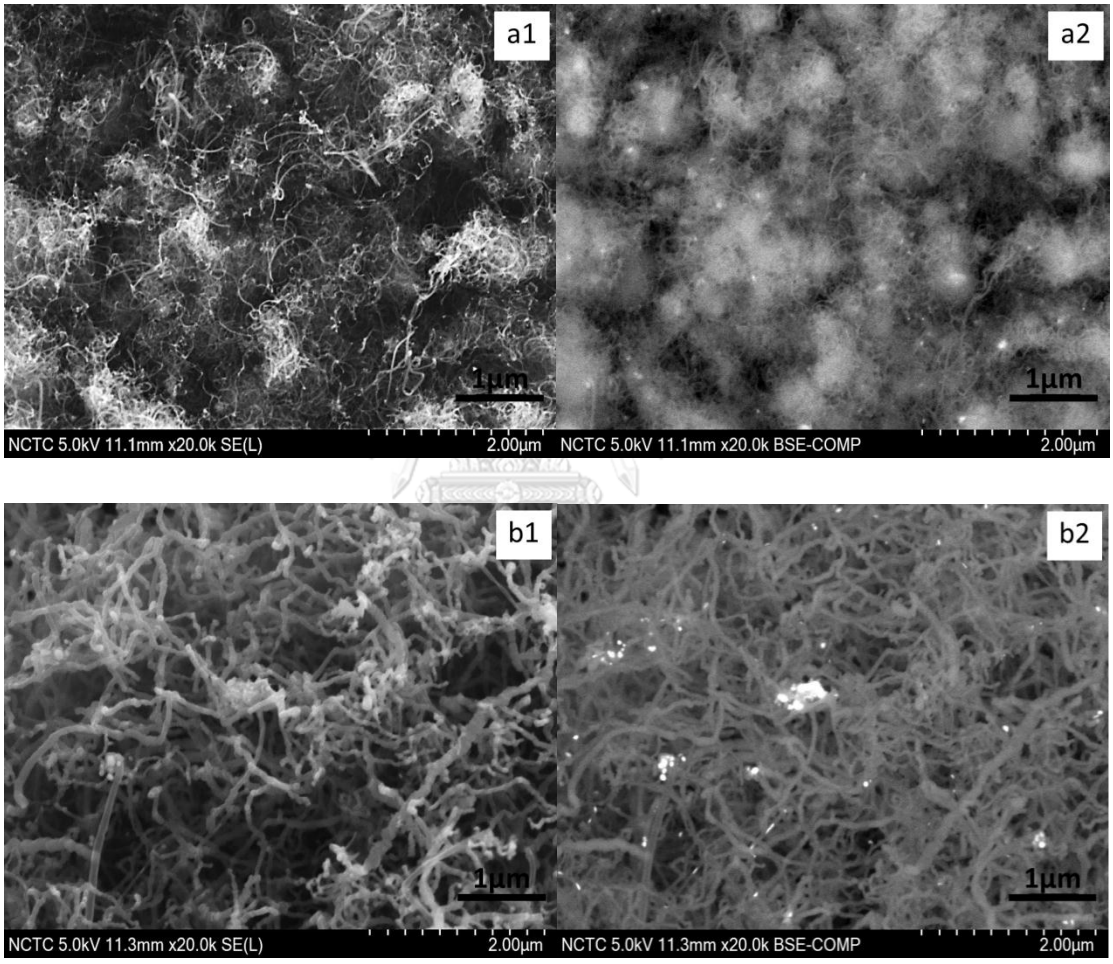

Fig. 4.8 FE-SEM images and BSC/FE-SEM images of (a1, a2) Commercial CNTs and (b1, b2) M-CNPs, respectively

Comparison of morphological appearance of commercial CNTs and M-CNPs was illustrated in **Fig. 4.8**. A field-emission scanning electron microscopy (FE-SEM), equipped with Back-scattered Electron Detector (BSC/FE-SEM) was employed the commercial CNTs in **Fig. 4.8 (a2)** that have the difference elements

form difference colors. There is the dispersion of element uniformly. The **Fig. 4.8 (b2)** was shown the difference elements form difference colors as the commercial CNTs, but there were the cluster of element that did not uniformly adheres on another element. Thus, this cluster of this element was the group of iron-cluster. This data will be support in FE-SEM/EDX.

Furthermore, a field-emission scanning electron microscopy with energy dispersive X-ray spectroscopy (FE-SEM/EDX) which were shown already in **Fig. 4.9**, was employed for verifying the correspondence of microstructure and elemental contend of M-CNPs taken from zone C. Found that, a main peak at 0.28 keV with 2 representing peak at 0.7 keV and 6.4 keV. These Spectrums confirm the main ingredients of carbon mixed with a small amount of Fe were illustrated.

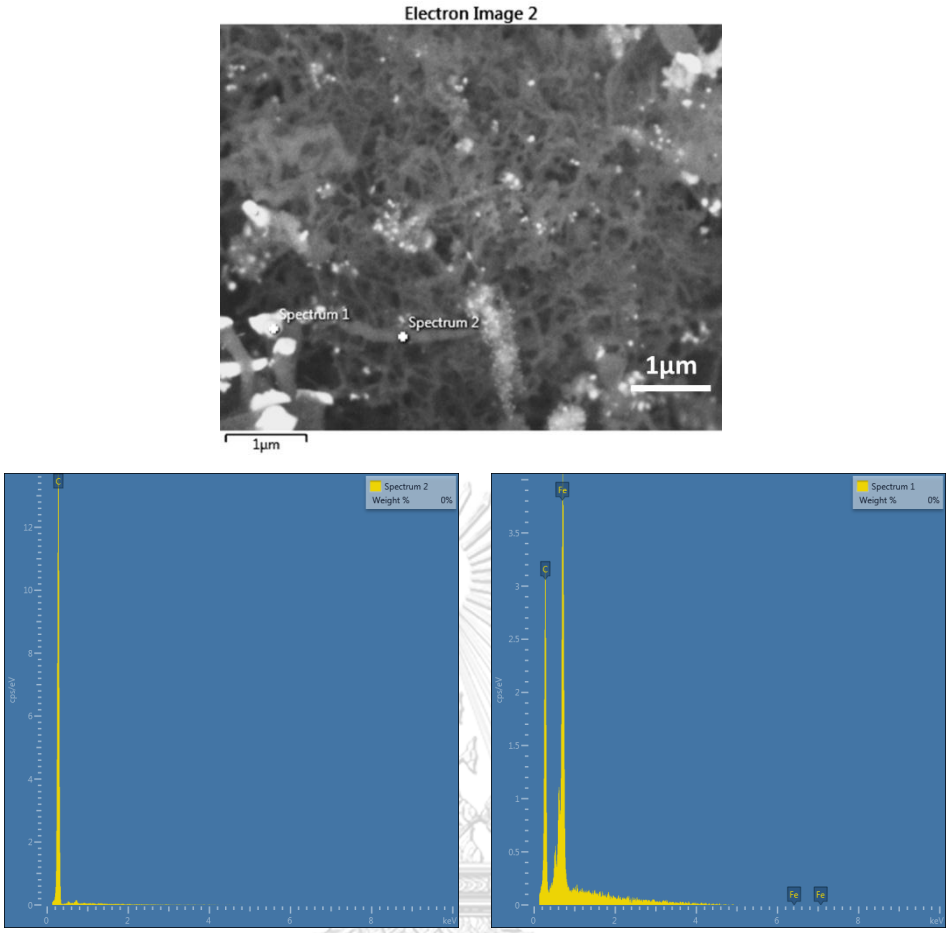

Fig.4.9 FE-SEM/EDX spectrum of M-CNPs

The result M-CNPs were subjected to transmission electron microscopy (TEM) used to show the multi-walled carbon nanotubes of commercial CNTs. In **Fig. 4.10**, there were the well-defined structure of inner hollow space and a high aspect ratio. They were determined about 10-20 nm of their diameter and 5-8 nm of wall thickness.

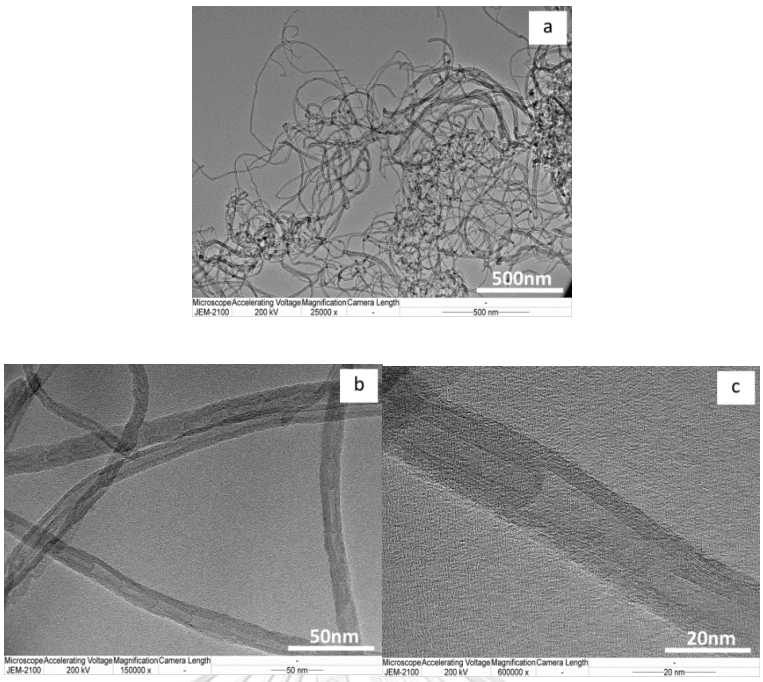

Fig. 4.10 TEM image of commercial CNTs at difference magnifications (a) 25,000× (b) 150,000× (c) 400,000×

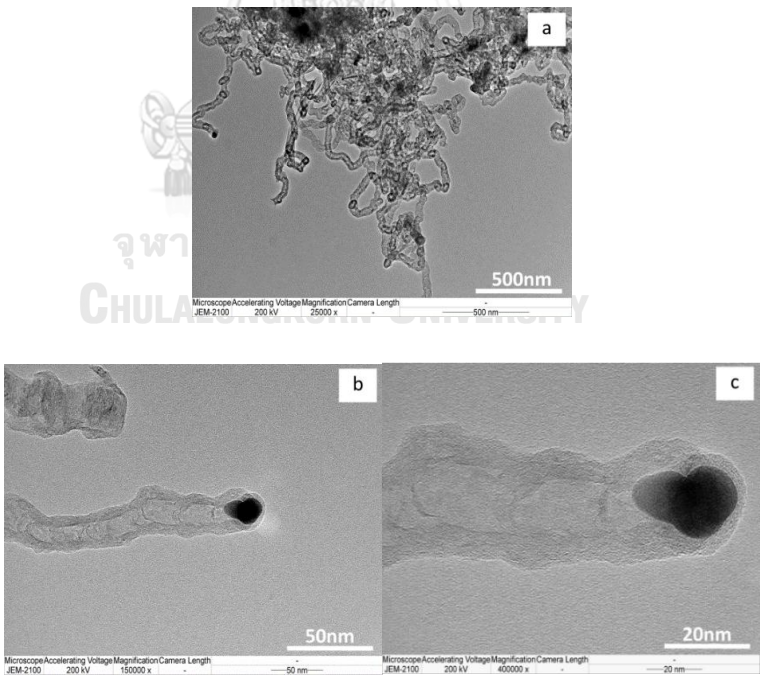

Fig. 4.11 TEM image of M-CNPs at difference magnifications (a) 25,000× (b) 150,000× (c) 400,000×

For the magnetic carbon nanoparticles (M-CNPs), which were synthesis via co-pyrolysis, contain mostly carbon nanotubular structure with some iron nanoparticles as a metal catalyst. They were also found to exhibits structure of inner hollow space as same as CNTs. In addition, the iron nanoparticles as an active catalyst that is widely used a catalyst to enhanced the isomerization reaction [20]. The acid-treated CNPs were the same as M-CNPs that had the metal particles, carbon nanoparticles and amorphous carbon in their structure. **Fig. 4.11 (b1), (b2) and (b3)** shows TEM image of M-CNPs M-CNPs were shown the presence of iron particles inside of tube in form of small spheres can be observed. In addition, the TEM images were confirmed that nanotubular structure was multi-walled layers. Most often, metal nanoparticles were encapsulated by carbon nanoparticles, they are obtained by adsorption of precursor during co-pyrolysis of lubricant oil and ferrocene mixtures [14].

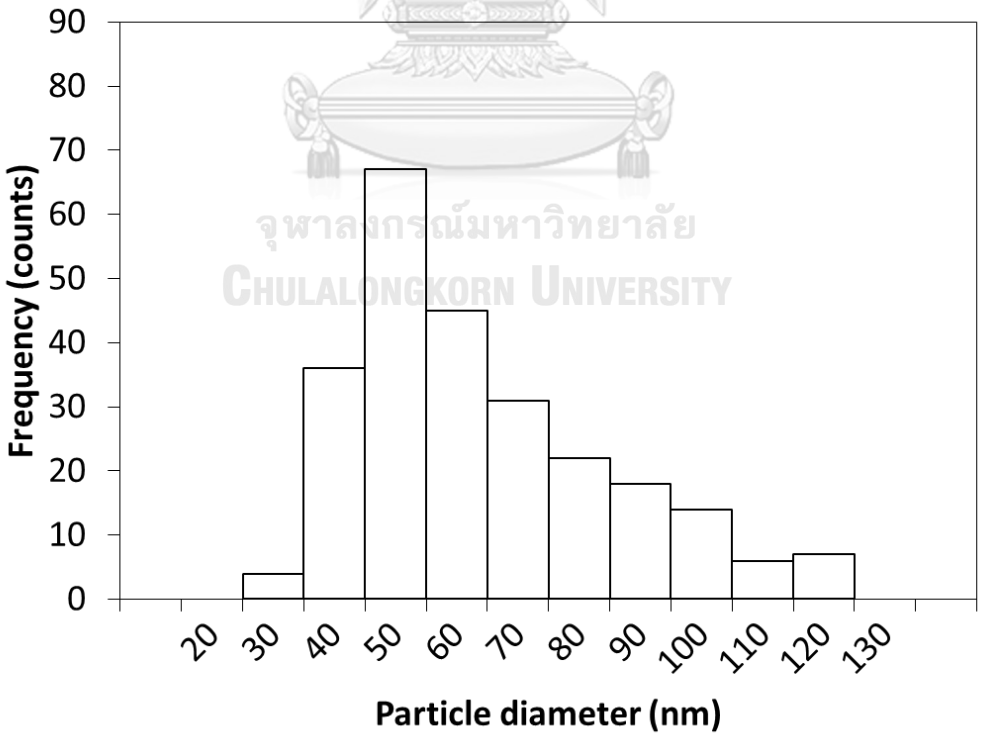

Fig. 4.12 Particles size distribution of M-CNPs

From the particles distribution of M-CNPs, They are obtained carbon nanoparticles that have surface area with diameters ranging from 25 to 125 nm as shown in **Fig. 4.12**. The highest of diameter equal the range of 50 nm.

4.2 Acid treatment of M-CNPs hybridized with 8M of nitric acid

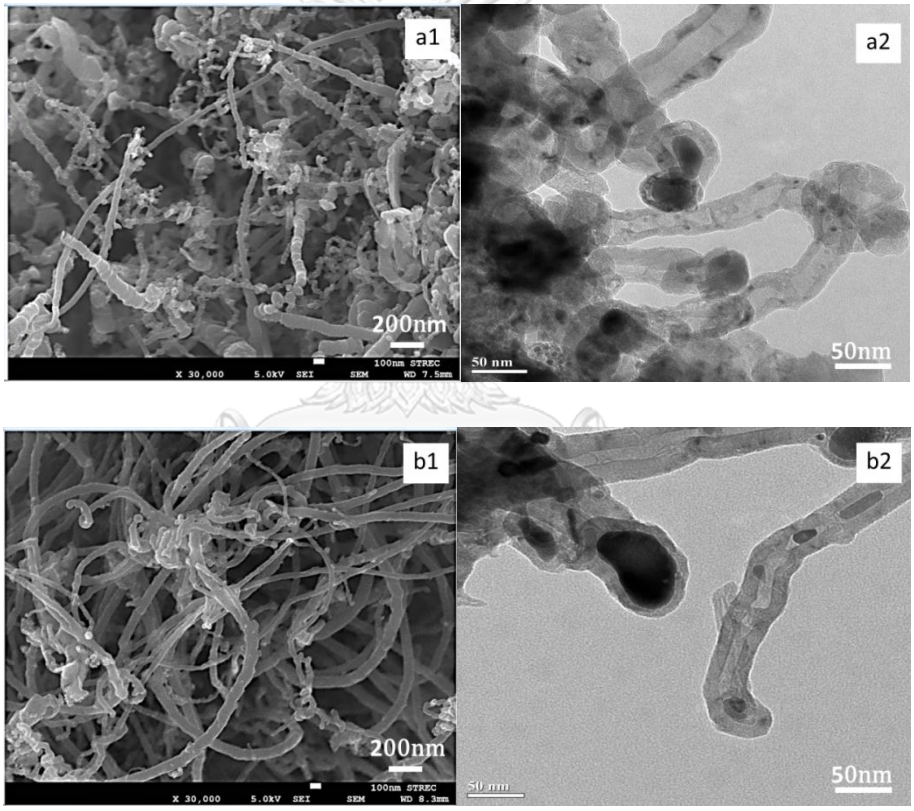

Fig. 4.13 SEM and TEM images of (a1, a2) M-CNPs and (b1, b2) acid-treated M-CNPs, respectively

Form **Fig. 4.13 (b1, b2)**, they were observed that the acid-treated M-CNPs could be removed the carbonaceous impurities and the iron compound. Thus, the impurity of external surface of acid-treated M-CNPs was cleaner than M-CNPs, but

the HNO_3 treatment did not affect the nanotubular structure because the acid could not be removed the iron particles in the tubular structure. Thus, the iron particles could be observed in the **Fig. 4.13 (b1, b2)** as same as the morphology of M-CNPs in **Fig. 4.13 (a1, a2)**.

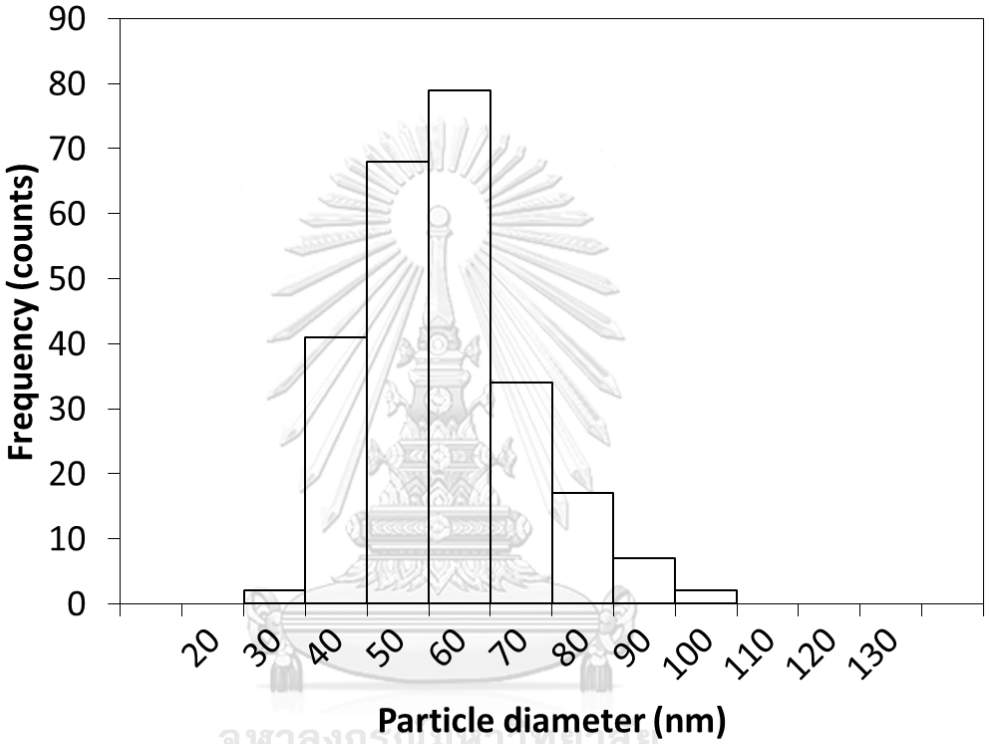

Fig. 4.14 Particle size distribution of Acid-treated M-CNPs

The surface of acid treatment M-CNPs has surface area with diameters in the range of 25 to 105 nm. This result is in agreement with the particle size distribution in **Fig. 4.14** that is less than the largest diameter of M-CNPs due to the removal impurities of metal particles and carbonaceous appeared from the production of the synthesis of M-CNPs [21]. The acid-treated M-CNPs the average particle diameter in the range of 60 nm was observed.

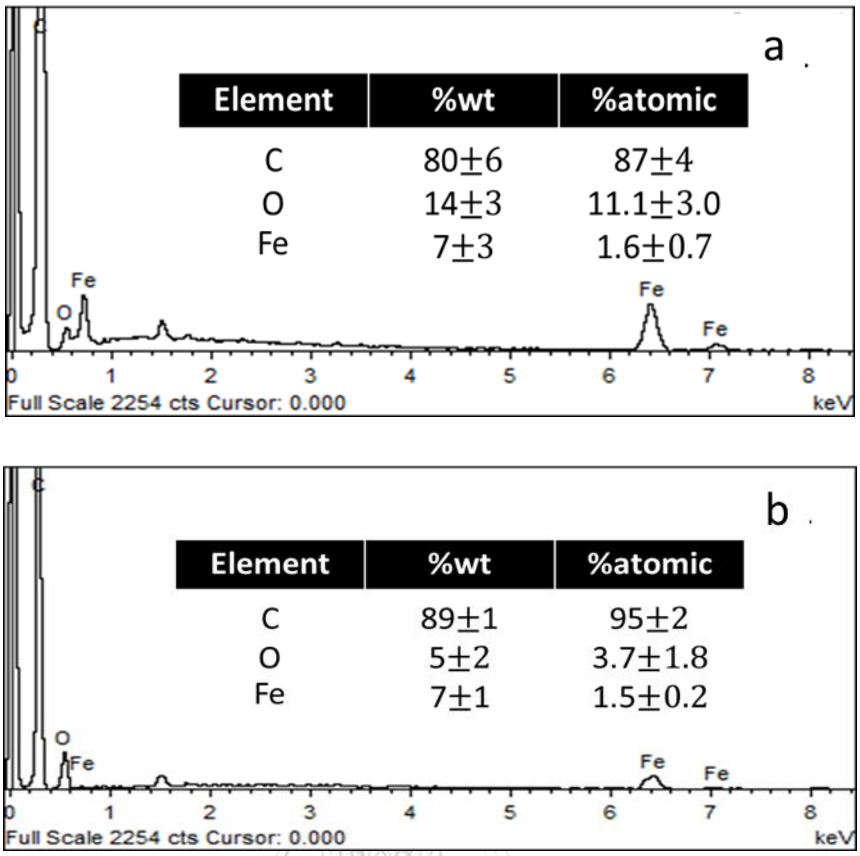

Fig. 4.15 The FE-SEM/EDX spectrum pattern of (a) M-CNPs and (b) Acid-treated M-CNPs

The EDX spectra, shown in **Fig. 4.15**, were employed the oxygen and iron percentages and carbon nanoparticles. The EDX results were indicate that O (5 and 14%wt and 3.7 and 11.1% atomic of M-CNPs and acid-treated M-CNPs, orderly) and Fe (7 and 7%wt and 1.5 and 1.6% atomic of M-CNPs and acid-treated M-CNPs, orderly). These were possibly distributed over the surface of C (89 and 80%wt and 95 and 87% atomic of M-CNPs and acid-treated M-CNPs, orderly) nanoparticles.

Table 4.5 the concentration of Fe in mg/L and mg/g catalyst from AAS

Samples	Concentration of Fe (mg/L)	Fe/catalyst (mg/g cat.)
M-CNPs	62.07	61
Acid-treated M-CNPs	5.50	5.3

Analysis by AAS in the residual liquid was demonstrated the elimination of 62.07 and 5.50 mg/L of iron with use 69% HNO_3 of M-CNPs and Acid-treated M-CNPs, respectively. For the concentration of Fe of CNTs as shown in **APPX.C** was 0.26mg/L, that could be the impurity of CNTs. As the concentration of Fe in commercial CNTs, M-CNPs and acid-treated M-CNPs, they were referred 0.23, 61 and 5.3 mg/1 g cat, respectively. The decreasing of the amount of iron, some iron compounds were dissolved in acid solution because of acid treatment.

Table 4.6 The Brunauer-Emmett-Teller (BET) surface area, total pore volume and average pore diameter of M-CNPs and the acid-treated M-CNPs

Samples	a_s,BET (m^2g^{-1})	Total pore volume (cm^3g^{-1})	Avg. pore diameter (nm)
M-CNPs	43±3	0.06±0.01	4.58±0.15
Acid-treated M-CNPs	44±1	0.06±0.02	5.84±1.92

The surface area from BET analysis was conducted on M-CNPs and acid-treated M-CNPs. The results were shown in **Table 4.6**. After M-CNP was treated with acid solution, surface area, total pore volume and average pore diameter a little increased because of removing the impurities, metal particles and other carbonaceous from M-CNPs. Because the decomposed particles of the feedstock in the high temperature were greater than the low temperature. Thus, the deposited carbon and iron particles were heavily blocked the pore on the surface of the product.

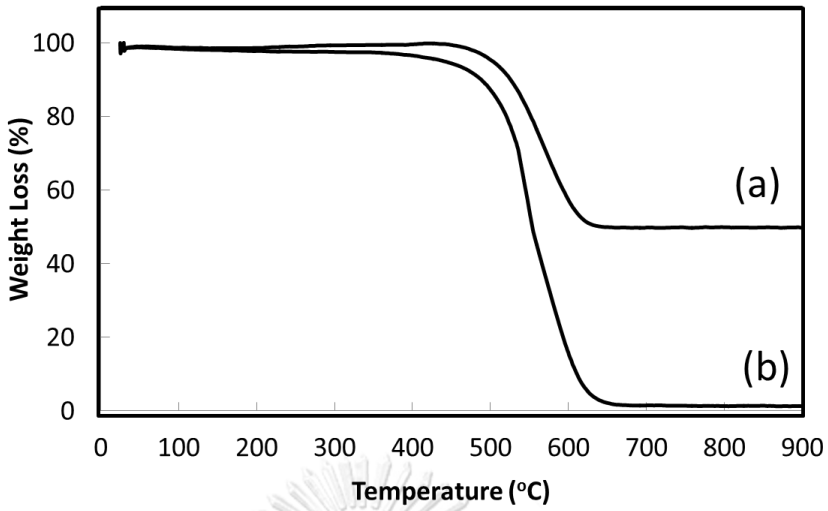

Fig.4.16 The Thermal stability of (a) the M-CNPs and (b) the acid-treated M-CNPs

TGA is a technique of thermal analysis in which the changing of weight of sample that is depend on the increasing temperature. The analyses of M-CNPs and acid-treated M-CNPs were carried out under the oxygen flow. When the temperature was increased, the samples were degraded by oxygen to be thermal oxidation and the residual at the end is generally iron compound as shown in **Fig. 16.** TGA of M-CNPs which was shown in **Fig. 16(a)**, was presented a starting degradation temperature of thermal oxidation of graphitic structure about 350°C and a final temperature about 620°C, with high degradation temperature about 550°C. The temperature of thermal oxidation of graphitic structure depends on the existing of impurities. Indeed, the impurities were degraded less than 350°C. Generally, commercial CNTs have the thermal oxidation in the range 500-700 °C and the amorphous are degraded at lower temperature (less than 400°C).[3] At the final of analyses 620°C, the residual content were about 50.4%. For acid-treated M-CNPs that the M-CNPs were treated by NHO_3 8M, the starting degradation temperature of thermal oxidation of and the temperature of the high degradation temperature is the same as M-CNPs, but the final temperature about 660°C. At the final of analyses

660ºC, the residual content were about 3.87%. As a result, M-CNPs and Acid-treated M-CNPs have a 49.6% and 96.13% of purity, orderly. Therefore, M-CNPs purity of impurity can be higher with acid treatment. For the residual weight measured is iron compound, the iron weight is higher than the mass detected by the AAS analysis as shown in **Table 4.5** because the thermal degradation can be decomposed carbon particle and left the residual iron in whole of M-CNPs and acid-treated M-CNPs. For AAS, it cannot be destroyed the overall carbon particles. Moreover, the HNO_3 8 M treatment was not damaged carbon nanostructure [22], as shown by SEM in **Fig. 4.13**, although amorphous carbon has been eliminated, as shown by Raman spectra in **Fig 4.17**.

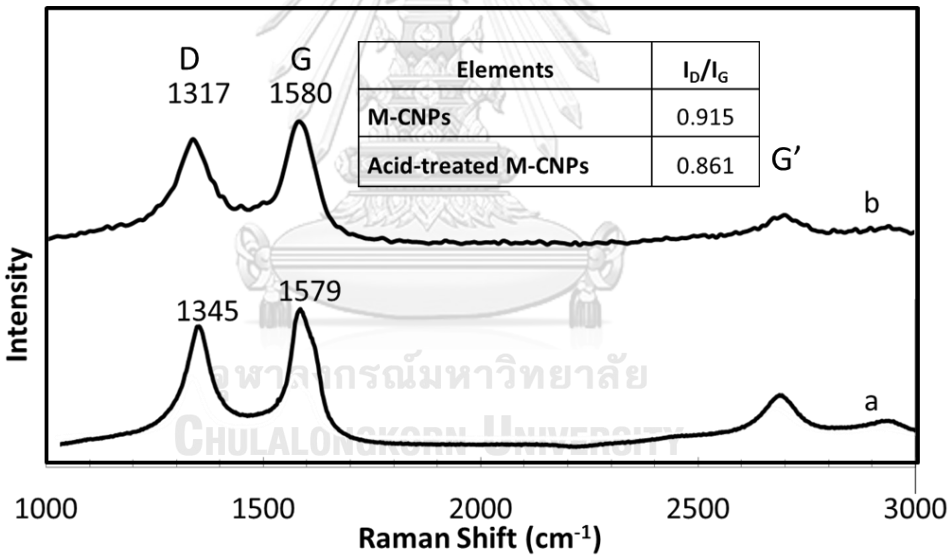

Fig. 4.18 Raman spectrum of (a) M-CNPs (b) Acid-treated M-CNPs

The M-CNPs and Acid treated M-CNPs were studied by Raman spectroscopy in **Fig. 4.18**. The Raman spectrum is very sensitive to variation of structural disorder in graphitic materials. The Raman spectra of graphite are consisted of 4 main bands, designed: D, G and G', as visualized by He-Ne laser (532 nm). The intensity of D represents the existence of defects and other effects induced

by any type of carbon. A ratio between the intensities of G and D bands (I_D/I_G) is used to determine the disorder and graphitic materials. An increase in I_D/I_G, there is more disorder structure that is higher proportion of sp^3 carbon. G' band with high intensity is high ordered nanographites. Raman spectra were showed a similar Raman Characteristic, the I_D/I_G was reduced with acid-treated M-CNPs and all peaks were narrower than M-CNPs. It could be implied that the corrosion of amorphous carbon was appeared. In another hand, the spectrum of acid-treated M-CNPs that were treated by HNO_3 8M showed a decrease in G' band intensity and a broadening of all other bands. These are shown that the oxygen-based functional groups in acid-treated M-CNPs [22]. Thus, the Raman spectra provide the data about the removal of amorphous and disorder structures from M-CNPs after acid treatment.

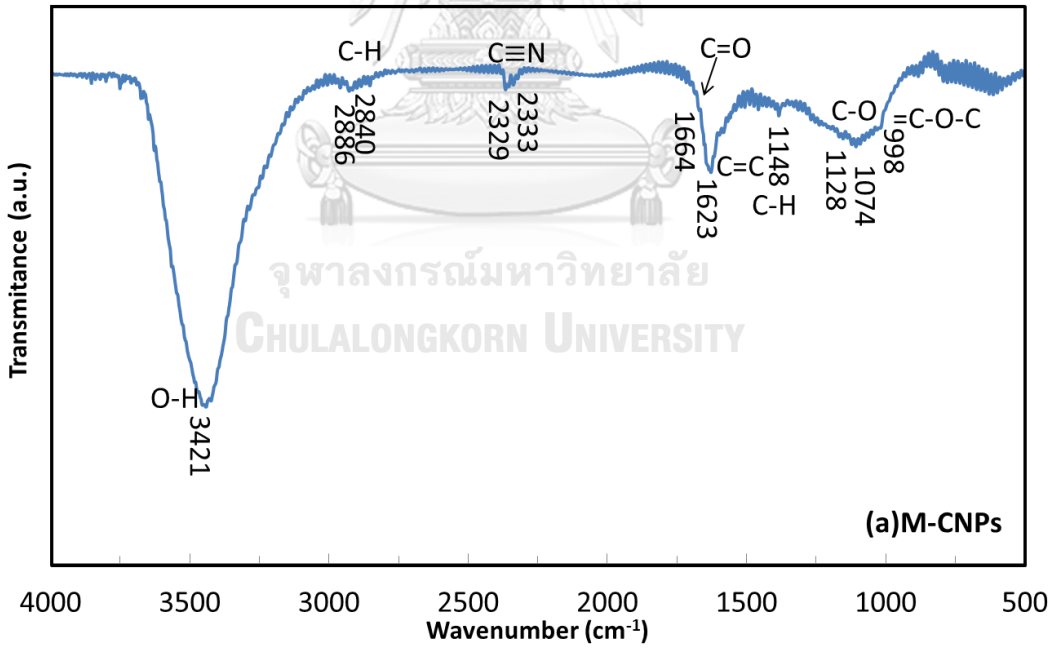

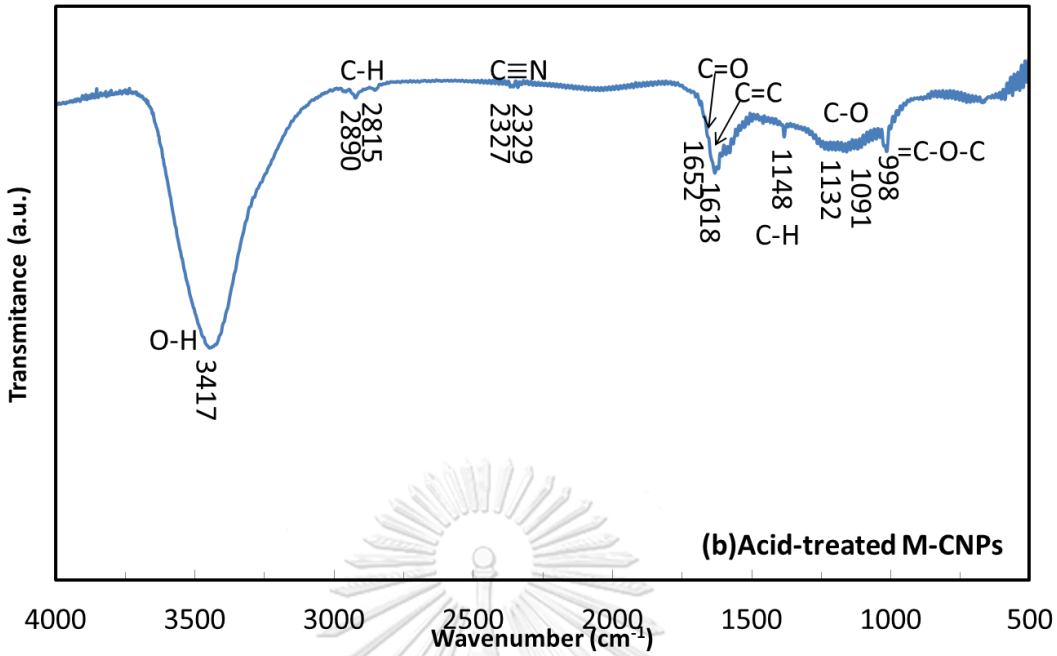

Fig. 4.19 FT-IR spectra of (a) M-CNPs and (b) acid-treated M-CNPs

Fourier transforms infrared (FT-IR) spectra of M-CNPs and acid-treated M-CNPs were obtained. From data of FT-IR and TEM, it was found that the iron particles inside M-CNPs and acid-treated M-CNPs were produced by co-pyrolysis that are consisted of carbon and iron in alpha structure, metallic and oxide nanoparticles. Generally, the oxide-iron was formed on the external surface of M-CNPs [22]. For acid-treated M-CNPs, the HNO_3 solution can adsorb on the nanotubes walls and oxide all amount of Fe^o to iron oxides. In addition, the acid-treated M-CNPs were oxidized to treat with HNO_3 that were increased the carboxylic group by the insertion of oxygen on nanoparticle surface.

According to oxidative treatment the proportion of OH to C=O bonds decrease because of carboxylic group presence as shown in **Table 4.7**.

Table 4.7 The ratio of intensity of OH and C=O of M-CNPs and acid-treated M-CNPs and acidity of M-CNPs and acid-treated M-CNPs from auto-titration

Samples	$I_{OH}/I_{C=O}$	Total acidity (mmol/g)
M-CNPs	4.25	0.019
Acid-treated CNPs	3.09	0.023

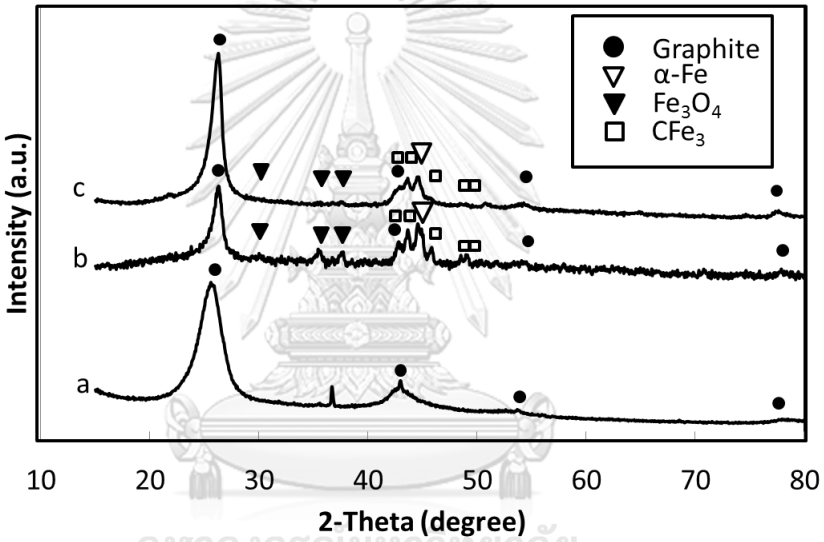

Fig. 4.20 XRD of (a) commercial CNTs, (b) M-CNPs and (c) acid-treated M-CNPs

The X-ray diffraction (XRD) analysis has been known as a powerful technique for characterizing the particle size. The XRD pattern of carbon, oxygen and iron were shown in the **Fig. 4.20** reveal a commercial CNTs, M-CNPs and acid-treated M-CNPs gave identical peak at 2θ = 26° that shown the carbon nanotubes diffraction. The Fe_3O_4 particles are identical peak at 2θ = 43°, 54° and 78°. The α-Fe particles are identical peak at 2θ = 45°. The CFe_3 particles are identical peak in

range 2θ = 42°-48° of M-CNPs and acid-treated M-CNPs. The strong reflections confirm the crystalline nature of the obtained M-CNPs were hybrid with iron and the iron with oxygen. This graph was presented the evidence of Fe_3O_4, α-Fe, and CFe_3 nanoparticle located inside and outer surface [23, 24].

4.3 Performance of M-CNPs and acid-treated M-CNPs for conversion of glucose to levulinic acid.

4.3.1 Effect of catalysts

Performance testing for conversion glucose by using commercial CNTs, M-CNPs and acid-treated M-CNPs

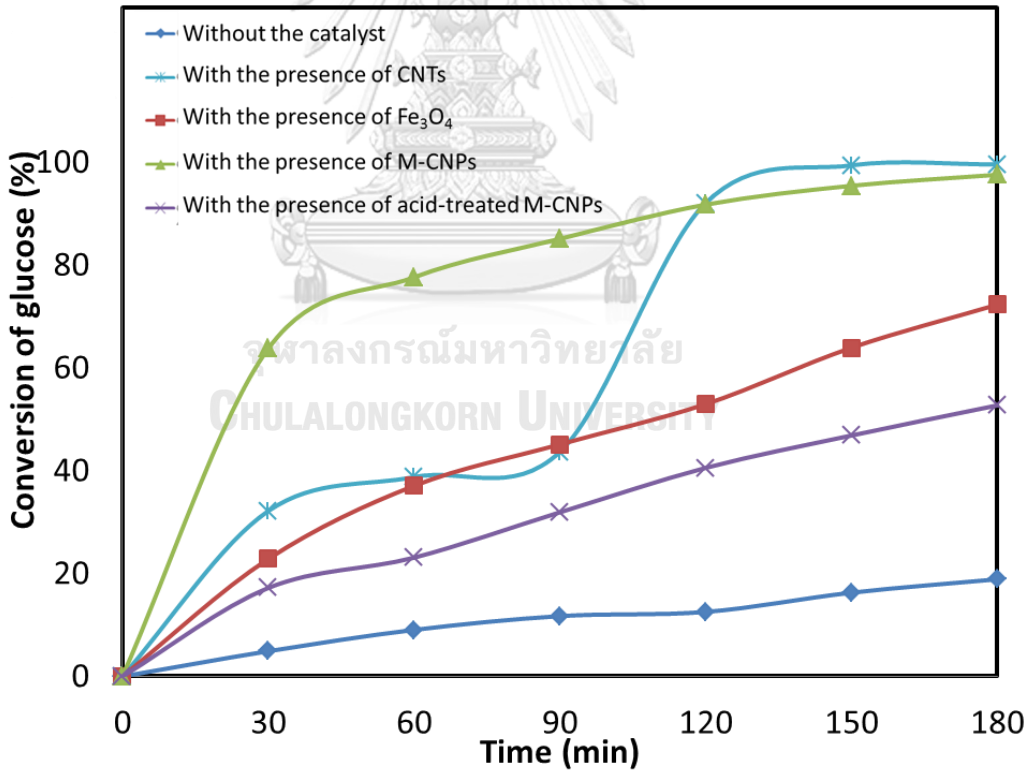

Fig.4.21 The conversion of glucose on the time

From the HPLC result, **Fig. 4.2** showns glucose conversion that was increased when the reaction time was increased with the absence catalyst, with the

presence of commercial CNTs, Fe_3O_4, Acid-treated M-CNPs and M-CNPs at 160°C. The higher conversion of glucose was observed with presence of M-CNPs over other conditions in 0-120 min of reaction time. In 30-120 min, the glucose conversion with the presence of M-CNPs and commercial CNTs were higher than glucose conversion with the presence of other catalyst. But the glucose conversion of the reaction with the presence of Fe_3O_4 and acid-treated M-CNPs were higher than the reaction with the absence of catalyst. It indicated that the commercial CNTs, Fe_3O_4, acid-treated M-CNPs and M-CNPs could be catalyst to convert glucose to other derivative substances. In addition, the glucose conversion of the reaction with the presence of M-CNPs was higher than the reaction with the presence of acid-treated M-CNPs. From the AAS data as shown in **Table 4.5** the amount of iron in the M-CNPs was higher than in the acid-treated M-CNPs. Thus, the amount of iron could be affected to conversion of glucose. Bhalkilar group (2015) found that Fe_3O_4 enhance the glucose conversion in hydrothermal reaction (low reaction temperature and pressure). The catalytic behavior was implied to promote the production of fructose. Catalytic glucose conversion with iron oxide was observed when the Fe_3O_4 was added, the fastest conversion of glucose with considerable amount of fructose as the intermediates for production levulinic acid. Thus, the isomerization of glucose to fructose can improved by adding Fe_3O_4 [25]. In addition, the morphological and spectroscopies of M-CNPs and acid-treated M-CNPs are the same properties as commercial CNTs. Thus, carbon nanotubular structure could enhance the conversion of glucose. In addition, conversion of glucose that was observed with the presence of commercial CNTs was promptly increased in the range of 90-120 min because the adsorption of product and by-product were strongly adsorbed on surface of commercial CNTs before 90 min of reaction time. Therefore, active sites of catalyst were deactivated and blocked by adsorbate. As a result, rate of glucose conversion was slightly increased. In case of reaction time above 90 min, glucose conversion was increased again because dispersion of glucose, catalyst, and liquid product were better from stirring in autoclave leading to improved mass transfer in the system [26].].

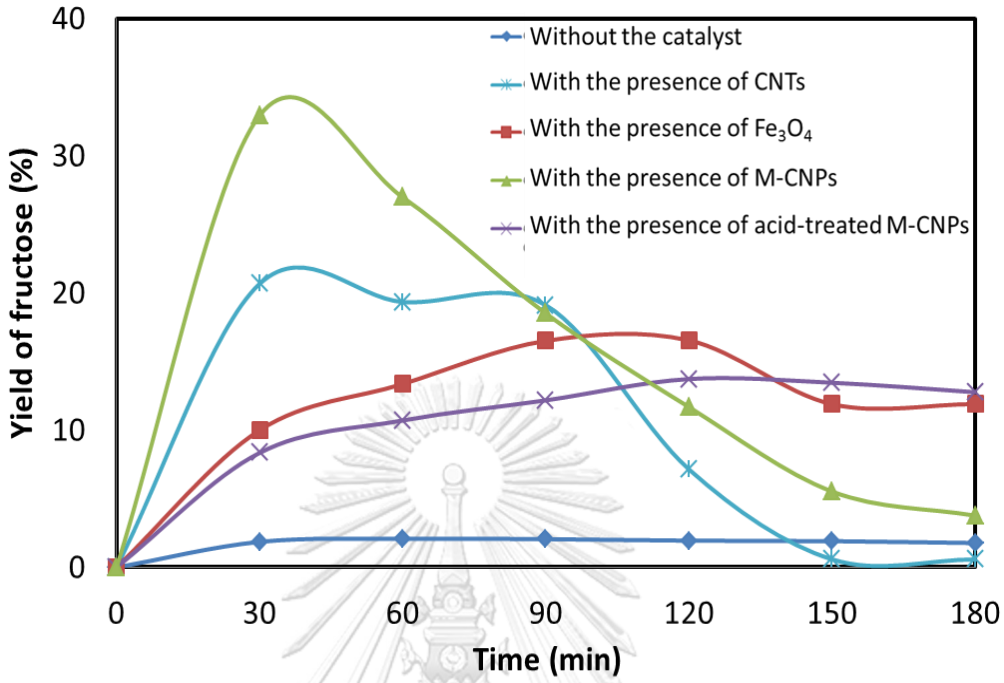

Fig. 4.22 Yield of fructose on the time

Fig. 4.22 shows fructose yield in the reaction with the absence catalyst, with the presence of commercial CNTs, Fe_3O_4, acid-treated M-CNPs and M-CNPs at 160°C. Fructose yield with presence of acid-treated M-CNPs was lower than with presence of M-CNPs because concentration of Fe in acid-treated M-CNPs was lower than M-CNPs. Moreover, fructose yield was increased in 0-60 min. Fructose yield was 26.98% with the presence of M-CNPs. That was the highest fructose yield than other catalyst because amount of Fe in M-CNPs was proper to produce fructose. Thus, the M-CNPs could be used catalyst for fructose production in 30 min at 160°C. When the reaction time was increased, the yield of fructose was decreased because of the consumption of fructose to produce other intermediates. Thus, fructose yield was depended on amount of Fe.

4.3.2 Effect of Amount of catalyst

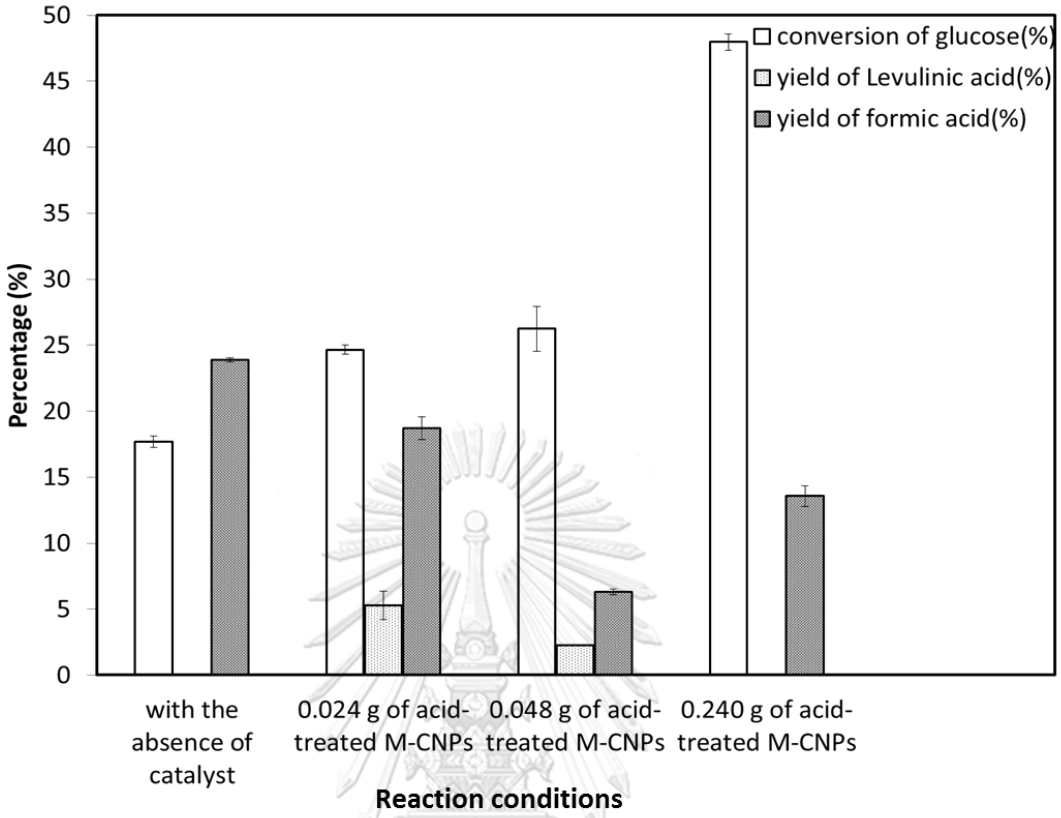

Fig. 4.23 Conversion of glucose, the yield of levulinic acid and the yield of formic acid from the condition that with the absence of catalyst, with the presence of 0.024, 0.048 and 0.24 g of acid-treated M-CNPs on 2hr of reaction time at 160ºC

From **Fig. 4.23**, it was shown conversion of glucose, yield of levulinic acid and yield of formic acid. This condition is the 0.900 g (0.2M) of glucose in 25 mL with the absence, with the presence of 0.024, 0.048 and 0.24 g of acid-treated M-CNPs at 160ºC for 2 hr. Conversion of glucose was increased when amount of catalyst was increased. Then, glucose conversion was depended on amount of Fe in catalyst. From previous study (4.3.1 the effect of catalysts), amount of Fe improved fructose production but it was not supported to produce levulinic acid. Fructose was substance that could be produce levulinic acid. In study of amount of catalyst effect, the yield of levulinic acid was interested and observed in reaction with the presence of acid-treated M-CNPs. Reaction with the presence of 0.024 g was obtained the highest yield of levulinic acid. Thus, the 0.024 g of acid-treated M-CNPs would be

used as catalyst to study effect of reaction time and temperature on production of levulinic acid. In addition, formic acid was found to parallel with levulinic acid. That was supported that interested pathway was appeared in autoclave. Trend of formic acid yield was same as levulinic acid yield.

4.3.3 Effect of reaction time

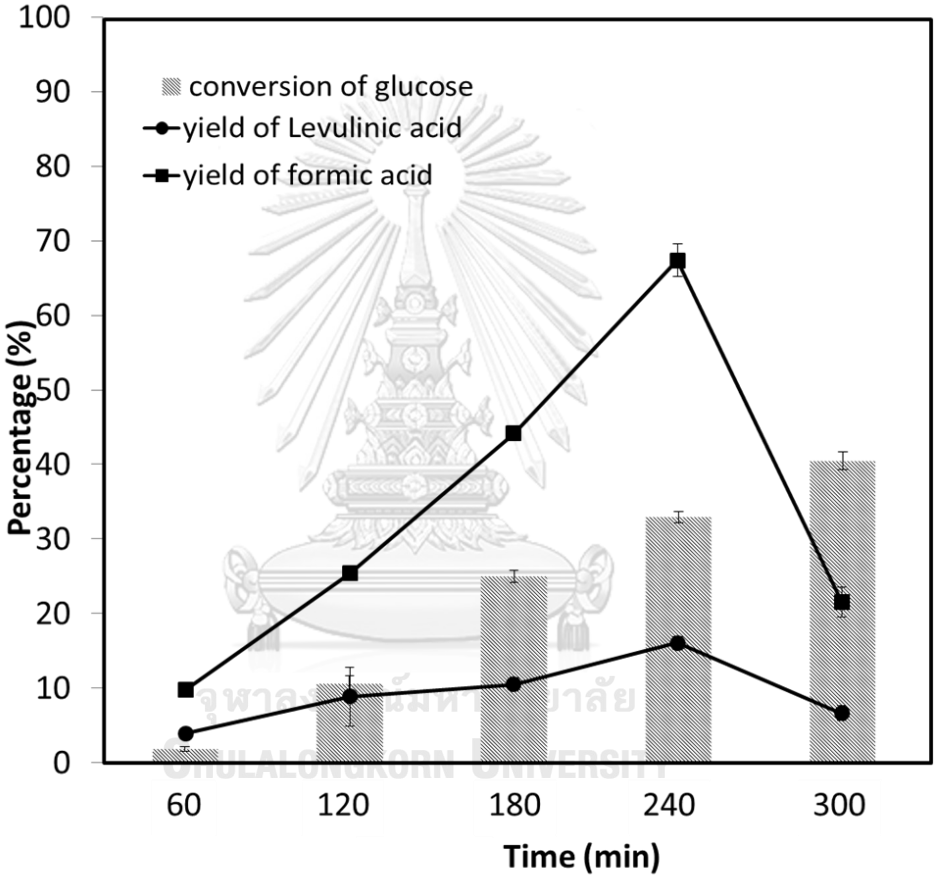

Fig. 4.24 Conversion of glucose, the yield of levulinic acid and the yield of formic acid from the condition with the presence of acid-treated M-CNPs on the time at 160ºC

Conversion of glucose, yield of levulinic acid and formic acid were shown in **Fig. 4.24**. This condition is the 0.900 g (0.2M) of glucose in 25 mL with the presence of 0.024 g of acid-treated M-CNPs at 160ºC and 60, 120,180,240 and 300 min of reaction time. Glucose conversion was increased when reaction time was increased.

The highest production of levulinic acid was observed at 240 min of reaction time. Levulinic acid and formic acid yield was 15.4% and 67.4%, orderly. Thus, optimal reaction time for levulinic acid production was 240 min. After 240 min, levulinic acid and formic acid yield were decrease because other derivative products were produced such as diol group, lactone, or ester [27]. Selectivity of levulinic acid and formic acid was 46.97 % and 14.60 % from 240 to 300 min. With increasing reaction time resulted in lower selectivity of levulinic acid. Thus, yield of levulinic acid depended on reaction time.

4.3.4 Effect of reaction Temperature

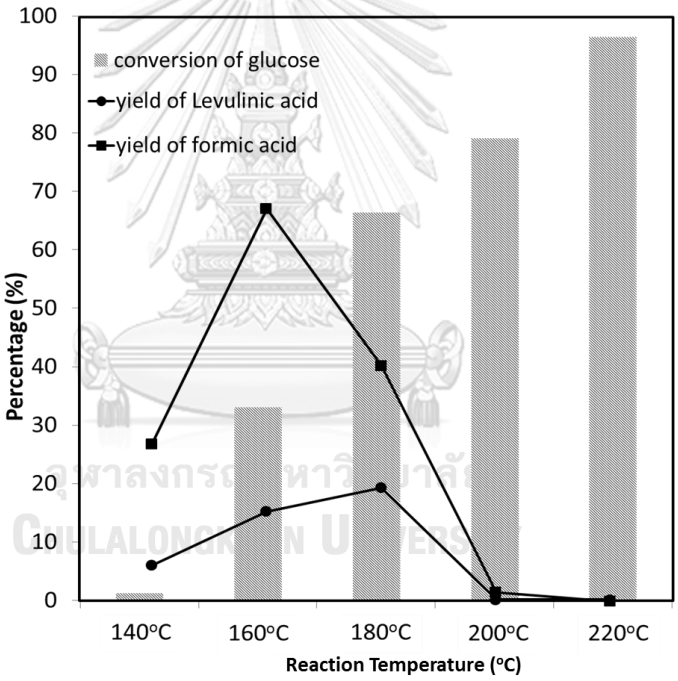

Fig. 4.25 Conversion of glucose, the yield of levulinic acid and the yield of formic acid from the condition with the presence of acid-treated M-CNPs on the reaction time at 140°C, 160°C and 180°C

Conversion of glucose, yield of levulinic acid and formic acid were shown in **Fig. 4.25**. This condition is 0.900 g (0.2M) of glucose in 25 mL with the presence of 0.024 g of acid-treated M-CNPs at 140, 160, 180, 200 and 220 °C for 240 min of

reaction time. Conversion of glucose increased when the reaction temperature increased. The maximum production of levulinic acid was appeared at 180ºC of reaction temperature. Yield of levulinic acid and formic acid was 19.5% and 40.5%, respectively. In addition, furfural, acetic acid, HMF and lactic acid could be investigated. Yield of livulinic acid, formic acid, furfural, acetic acid, HMF and lactic acid was 17.19%, 6.97%, 2.81%, 7.70%, 21.87%, 13.55% and 27.49%, respectively (calculated by number of carbon atom of glucose and products). In term of selectivity of levulinic acid, formic acid, furfural, acetic acid, HMF and lactic acid was 21.36%, 7.68%, 2.96%, 8.64%, 31.53%, 19.31% and 39.18%. Thus, optimal temperature for levulinic acid production was 180ºC. In addition, levulinic acid and formic acid yield were decreased because side reactions were occurred with increasing temperature [27]. They found that when the temperature was changed from 170-190ºC, levulinic acid formation was decreased as shown in **Fig. 4.26**

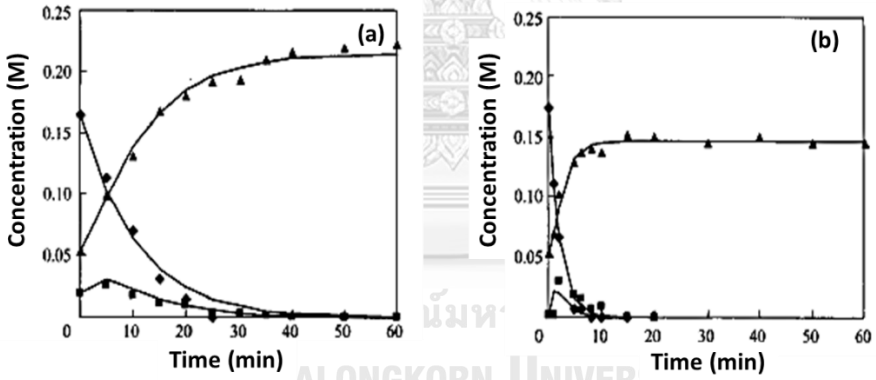

Fig. 4.26 The experiment and predict concentration of products generated during the 5% H_2SO_4 at (a) 170ºC and (b) 190ºC [27]

Levulinic acid and formic acid yields were decreased because glucose, HMF or levulinic acid were produced humic side reaction and decomposition product such as CO_2, H_2O at 200 and 220ºC of reaction temperature [27].

Chapter 5

Conclusion

5.1 Synthesis of M-CNPs hybridized with Fe nanoparticles via co-pyrolysis of lubricant oil and ferrocene

M-CNPs co-exiting with Fe nanostructures can be synthesized by Co-pyrolysis using lubrication oil and ferrocene. In this study, decomposition was appeared at 500^{o}C and product formation at 900 ^{o}C temperature. According to microscopic and spectroscopic analyses of the product, collected from the highest temperature location, the synthesized CNPs contain almost the same graphitic content as that of commercial CNTs. Due to the presence of Fe nanostructure, it implied that that the synthesized CNPs can be employed as catalyst.

5.2 Acid treatment of M-CNPs hybridized with 8M of nitric acid

Acid treatment of M-CNPs could provide functional groups on their surfaces which could affect their catalytic activities. Pristine M-CNPs and acid-treated M-CNPs could be used as heterogeneous catalysts for converting glucose to some derivatives.

5.3 Performance of the M-CNPs and acid-treated M-CNPs for conversion of glucose to levulinic acid was conducted.

Pristine M-CNPs and acid-treated M-CNPs could be used as heterogeneous catalyst for glucose conversion to some derivatives. The presence of Fe nanoparticles in M-CNPs could enhance the conversion of glucose and the production of fructose.

Pristine M-CNPs achieved high glucose conversion of 97.58% (by mole) and fructose yield of 26.98% (by mole).

Acid treated M-CNPs obtained 66.29% (by mole) of glucose conversion and 19.52% (by mole) of levulinic acid yield. The optimal condition for levulinic acid production from glucose was obtained at 0.900 g (0.2M) of glucose, 0.024 g of acid-treated M-CNPs, 180 ^{o}C of operating temperature.

5.4. Suggestion

Acid-treated M-CNPs will be effect of concentration of acid solution for carbon catalysts. For acid treatment of the carbon catalyst, effect of acid solution concentration for acid treatment of carbon catalysts will be examined. These carbon based catalysts will probably be as good as other catalysts that are supported on zeolite or alumina oxide.

REFERENCES

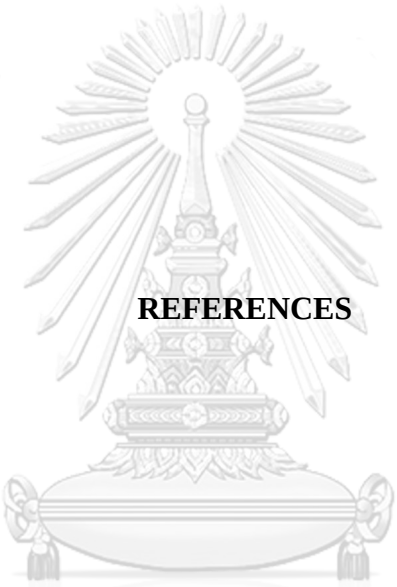

[1] C.H. Zhou, X. Xia, C.X. Lin, D.S. Tong, J. Beltramini, Chem Soc Rev 40 (2011) 5588-5617.
[2] A. Mukherjee, M.-J. Dumont, V. Raghavan, Biomass and Bioenergy 72 (2015) 143-183.
[3] M. Kumar, Y. Ando, Journal of Nanoscience and Nanotechnology 10 (2010) 3739-3758.
[4] A.S. Kumar, S. Sornambikai, L. Deepika, J.-M. Zen, Journal of Materials Chemistry 20 (2010) 10152.
[5] D.M. Webster, P. Sundaram, M.E. Byrne, Eur J Pharm Biopharm 84 (2013) 1-20.
[6] T. Charinpanitkul, N. Sano, P. Puengjinda, J. Klanwan, N. Akrapattangkul, W. Tanthapanichakoon, Journal of Analytical and Applied Pyrolysis 86 (2009) 386-390.
[7] M.J. Fuentes, R. Font, M.F. Gómez-Rico, I. Martín-Gullón, Journal of Analytical and Applied Pyrolysis 79 (2007) 215-226.
[8] D.J. Hayes, S. Fitzpatrick, M.H.B. Hayes, J.R.H. Ross, Biorefineries-Industrial Processes and Products, Wiley-VCH Verlag GmbH, 2008, pp. 139-164.
[9] N. Ya'aini, N.A.S. Amin, S. Endud, Microporous and Mesoporous Materials 171 (2013) 14-23.
[10] N.A.S. Ramli, N.A.S. Amin, Applied Catalysis B: Environmental 163 (2015) 487-498.
[11] I. Agirrezabal-Telleria, I. Gandarias, P.L. Arias, Catalysis Today 234 (2014) 42-58.
[12] R. Weingarten, Y.T. Kim, G.A. Tompsett, A. Fernández, K.S. Han, E.W. Hagaman, W.C. Conner, J.A. Dumesic, G.W. Huber, Journal of Catalysis 304 (2013) 123-134.
[13] N. Ya'aini, N.A. Amin, M. Asmadi, Bioresour Technol 116 (2012) 58-65.
[14] P.P. Upare, J.-W. Yoon, M.Y. Kim, H.-Y. Kang, D.W. Hwang, Y.K. Hwang, H.H. Kung, J.-S. Chang, Green Chemistry 15 (2013) 2935.
[15] A. Moisala, A.G. Nasibulin, E.I. Kauppinen, Journal of Physics: Condensed Matter 15 (2003) S3011-S3035.
[16] F. Avilés, J.V. Cauich-Rodríguez, L. Moo-Tah, A. May-Pat, R. Vargas-Coronado, Carbon 47 (2009) 2970-2975.
[17] H. Hu, B. Zhao, M.E. Itkis, R.C. Haddon, The Journal of Physical Chemistry B 107 (2003) 13838-13842.
[18] Martı, x, M.T. nez, M.A. Callejas, A.M. Benito, M. Cochet, T. Seeger, A. Ansón, J. Schreiber, C. Gordon, C. Marhic, O. Chauvet, J.L.G. Fierro, W.K. Maser, Carbon 41 (2003) 2247-2256.
[19] V. Datsyuk, M. Kalyva, K. Papagelis, J. Parthenios, D. Tasis, A. Siokou, I. Kallitsis, C. Galiotis, Carbon 46 (2008) 833-840.

[20] K.U. Lee, M.J. Kim, K.J. Park, M. Kim, O.J. Kwon, J.J. Kim, Materials Letters 125 (2014) 213-217.
[21] G. Malgas, C. J. Arendse, N. Cele, F. Cummings, Effect of mixture ratios and nitrogen carrier gas flow rates on the morphology of carbon nanotube structures grown by CVD, 2008.
[22] E.R. Edwards, E.F. Antunes, E.C. Botelho, M.R. Baldan, E.J. Corat, Applied Surface Science 258 (2011) 641-648.
[23] W. Chen, X. Pan, M.-G. Willinger, D.S. Su, X. Bao, Journal of the American Chemical Society 128 (2006) 3136-3137.
[24] P. Mahanandia, P.N. Vishwakarma, K.K. Nanda, V. Prasad, K. Barai, A.K. Mondal, S. Sarangi, G.K. Dey, S.V. Subramanyam, Solid State Communications 145 (2008) 143-148.
[25] A. Bhalkikar, Z.C. Gernhart, C.L. Cheung, Journal of Nanomaterials 2015 (2015) 1-8.
[26] P.P. Upare, D.W. Hwang, Y.K. Hwang, U.H. Lee, D.-Y. Hong, J.-S. Chang, Green Chemistry 17 (2015) 3310-3313.
[27] D.W. Rackemann, W.O.S. Doherty, Biofuels, Bioproducts and Biorefining 5 (2011) 198-214.

APPENDIX

APPENDIX A

Calibration curve of Glucose, fructose, Levulinic acid and formic acid for HPLC analyzer

Calibration curve of glucose, fructose, Levulinic acid and formic acid had to be done. Firstly, the standard solution was prepared the various amounts of standard substances in the deionized water. In order to make the calibration curve of each concentration, 0.1, 0.2, 0.3, 0.4 and 0.5 M of standard glucose were injected in the HPLC analyzer.

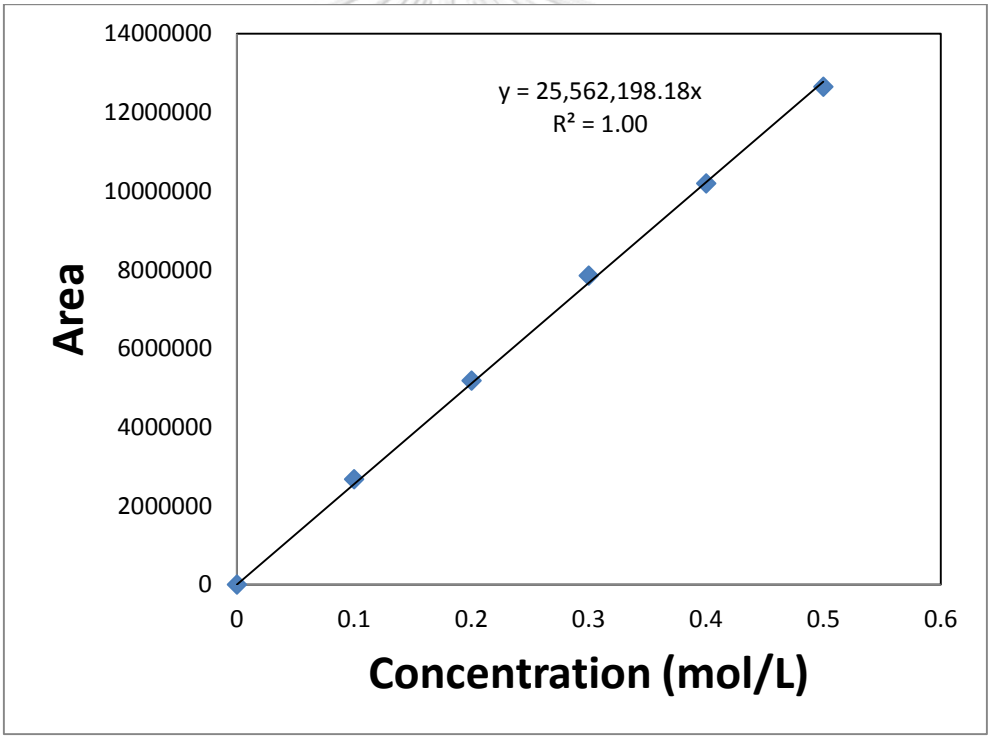

Fig. A1 Calibration curve of glucose

In the standard fructose calibration curve of each concentration 0.5, 2.0, 20 and 50 mg/mL of standard fructose were injected in the HPLC analyzer.

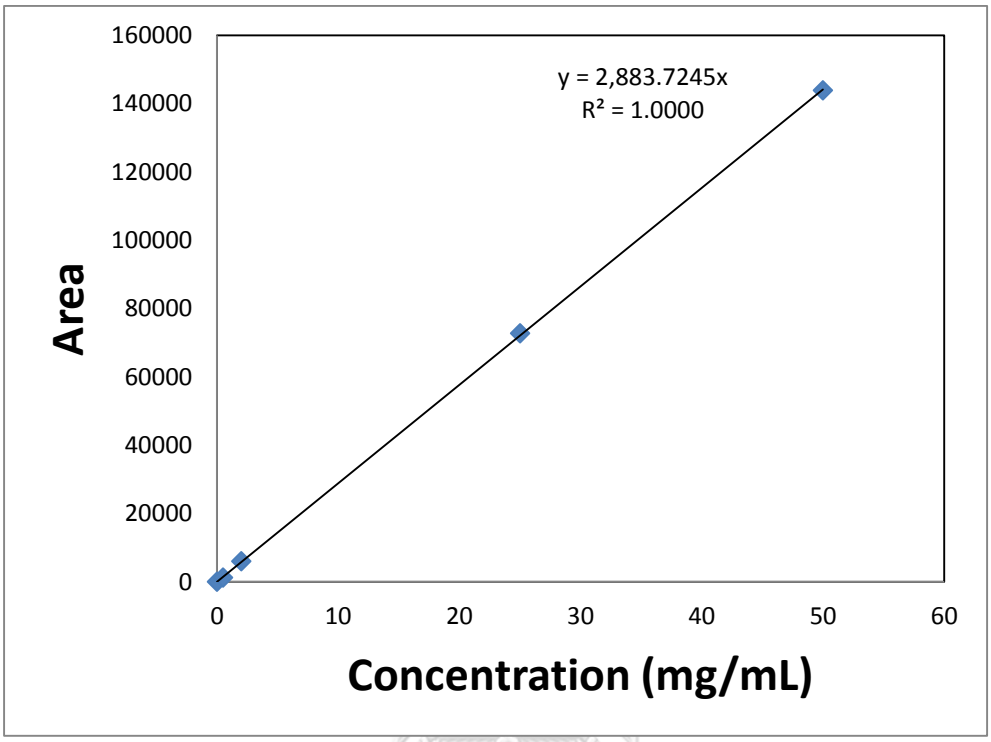

Fig. A2 Calibration curve of fructose

In the standard levulinic acid and formic acid calibration curve of each concentration 0.05, 0.5, 2.0, 20 and 50 mg/mL of standard levulinic acid and formic acid in de-ionized water were injected in the HPLC analyzer.

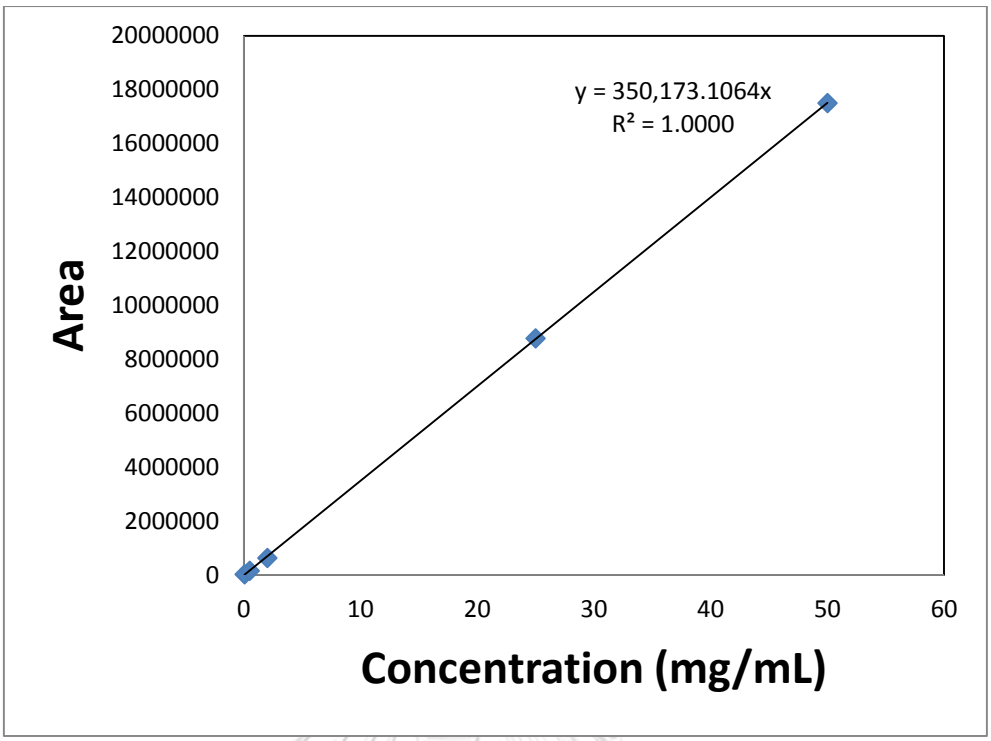

Fig. A3 Calibration curve of levulinic acid

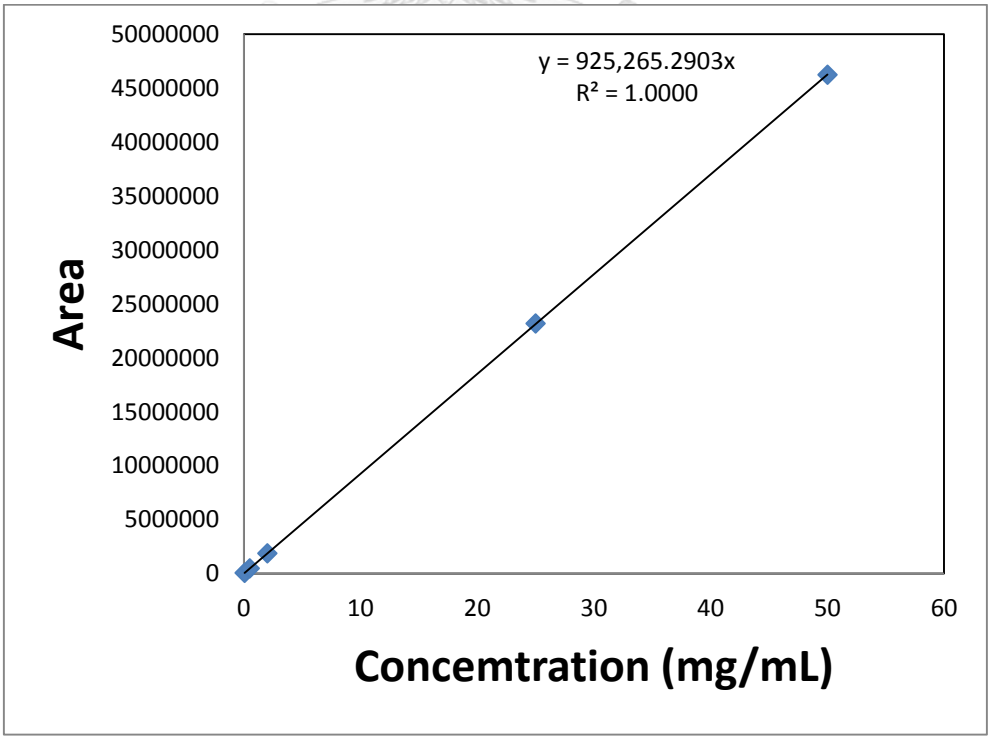

Fig. A4 Calibration curve of formic acid

APPENDIX B

Calculation the concentration from data of HPLC

Ex. Concentration of glucose

From calibration curve in APPX.A1, y = 25,562,198.18x is the equation to convert the area to the concentration. Due to the unit of concentration of glucose in calibration is mol/dm^3. We can calculate:

Assume: The area data from HPLC result: 2807308 = y

Form y = 25,562,198.18x

Substitute y=2807308 ; 2807308 = 25,562,198.18x

x = 0.109822637 mol/dm^3

Ex. Concentration of fructose

From calibration curve in APPX.A2, y = 2,883.7245x is the equation to convert the area to the concentration. Due to the unit of concentration of fructose in calibration is mg/mL. We can calculate:

Assume: The area data from HPLC result: 426469 = y

Form y = 2,883.7245x

Substitute y= 426469 ; 426469 = 25,562,198.18x

x = 3.149906567 mg/mL

Divide by MW. of fructose

MW. of fructose =180 mg/mL; x = 0.017499481 mol/mL

APPENDIX C

Characteristic of commercial CNTs from AAs and FT-IR

Table C1 The concentration of Fe in mg/L and mg/1grams catalyst from AAS

Samples	Concentration of Fe (mg/L)	Concentration of Fe (mg/1 g cat.)
Commercial CNTs	0.26	0.23

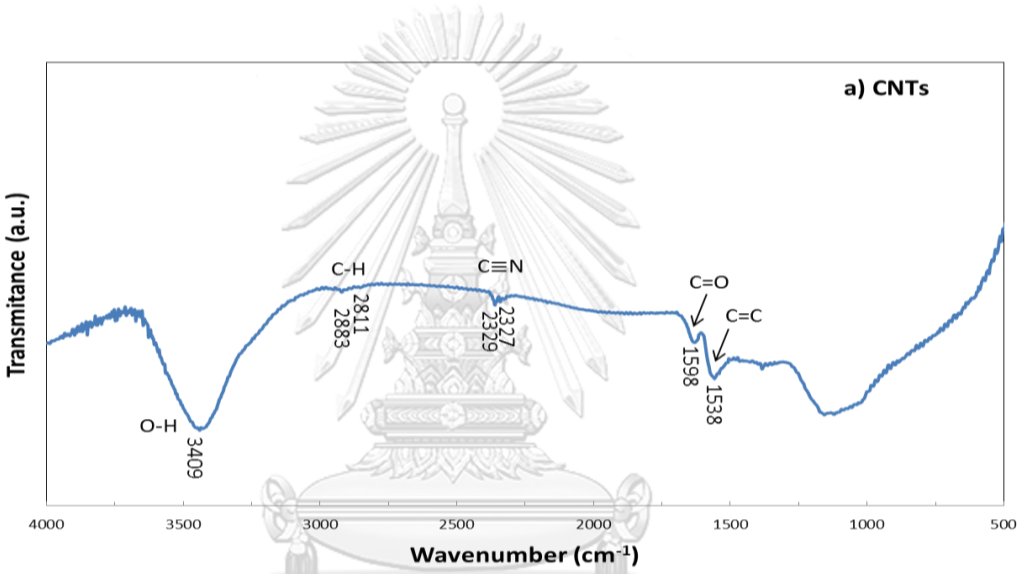

Fig. C1 FT-IR spectra of (a) commercial CNTs

Table C2 The ratio of OH and C=O of commercial CNTs

Component	$I_{OH}/I_{C=O}$
Commercial CNTs	3.67

APPENDIX D

Catalytic Path ways

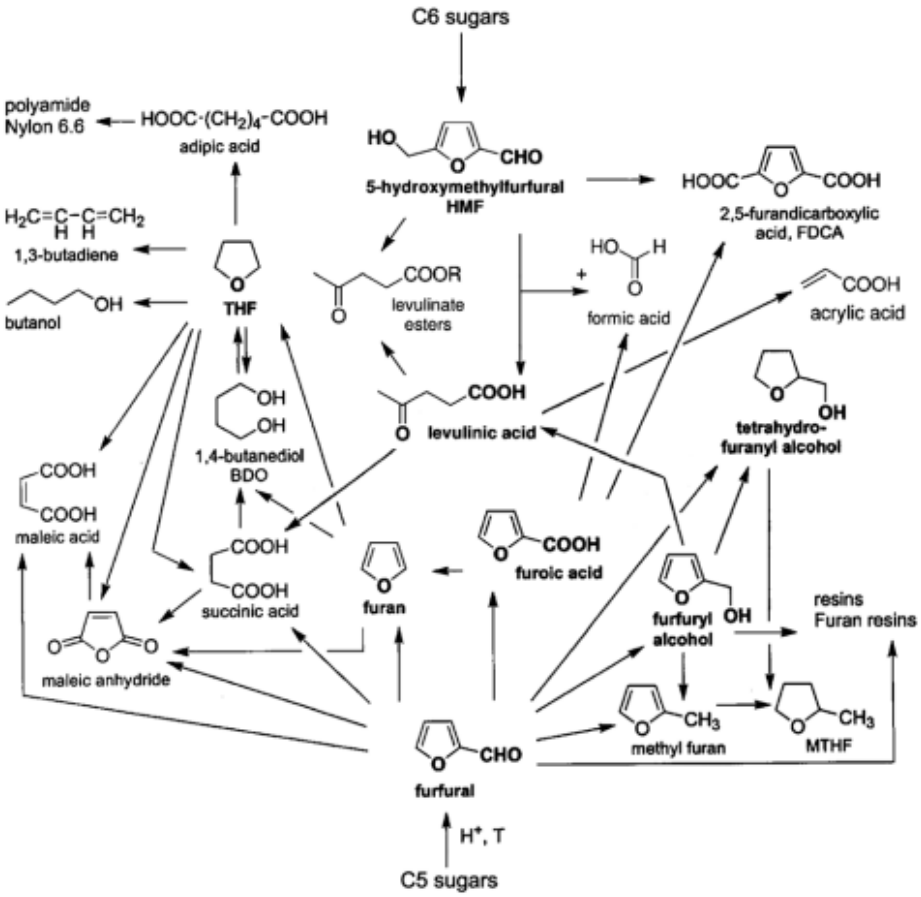

Fig. D1 Catalyst path way of C6 and C5 sugar

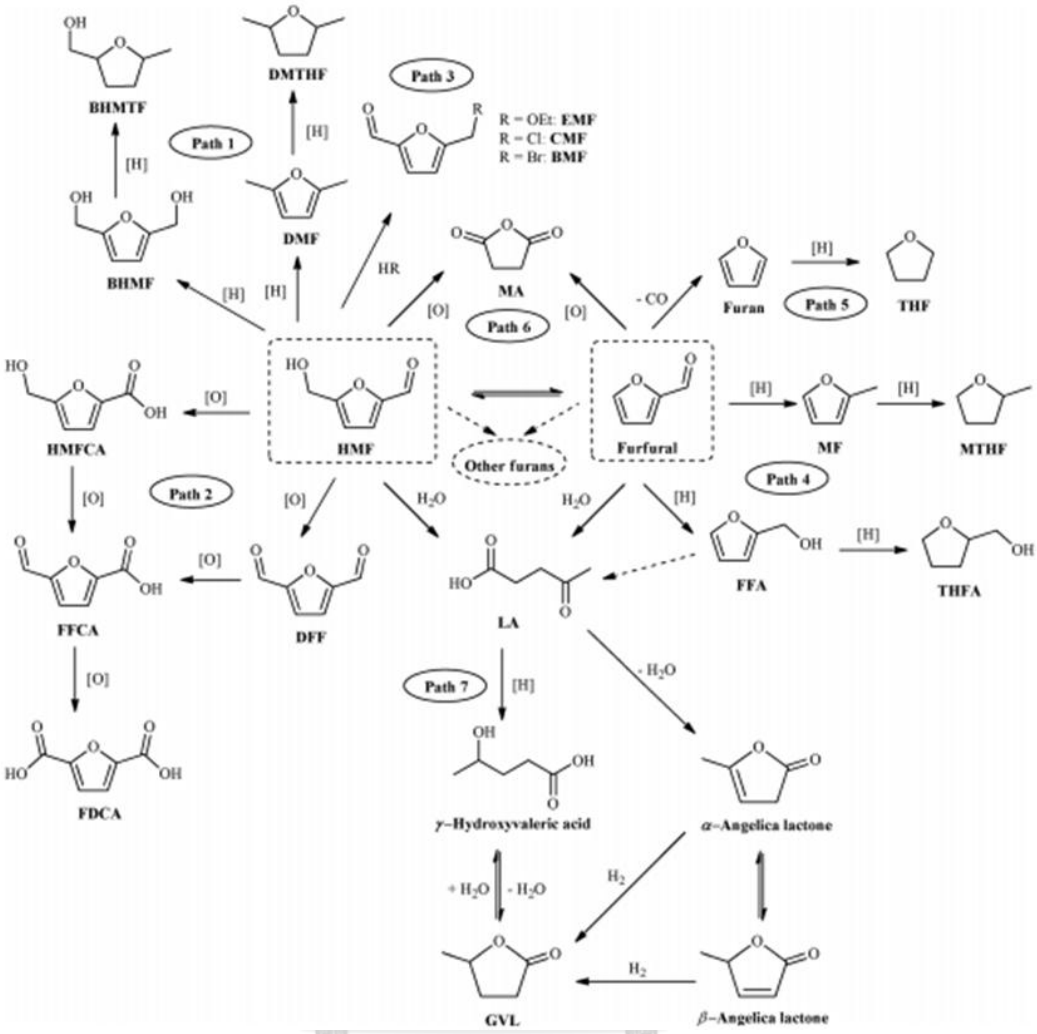

Fig. D2 Catalyst path way of C6 and C5 sugar

VITA

Ms. Jirarat Kaewngam was born on July 16th, 1990 in Bangkok, Thailand. She obtained her Bachelor from Department of Chemistry, Faculty of Science, Mahidol University in 2012 and continued her Master in Center of Excellence in Particle Technology (CEPT), Department of Chemical Engineering, Faculty of Engineering, Chulalongkorn University.